REPORT 1226

A METHOD FOR THE DESIGN OF SWEPTBACK WINGS WARPED TO PRODUCE SPECIFIED FLIGHT CHARACTERISTICS AT SUPERSONIC SPEEDS [1]

By Warren A. Tucker

SUMMARY

One of the problems connected with the sweptback wing is the difficulty of controlling the location of the center of pressure and hence the pitching moment. A method is presented for designing a wing to be self-trimming at a given set of flight conditions. Concurrently, the spanwise distribution of load on the wing is made to be approximately elliptical, in an effort to maintain low wing drag.

These flight characteristics are achieved by warping the wing out of a plane. The required warp is determined by the values of the coefficients of a four-term series describing the pressure distribution; these values in turn are determined from four conditions on the lift, pitching moment, and spanwise load distribution.

The method is directly applicable to several wing plan forms, including the triangle and the sweptback plan form with finite tips, under the restriction that the leading edge must be subsonic and the trailing edge must be supersonic. The application to any specific problem is simplified to a routine computational procedure by the presentation of certain basic data in tabular form. A discussion is given of some points to be considered in the application of the method to a practical case, and several representative examples are worked out. The resulting wings are shown to be ones which might practicably be built.

INTRODUCTION

The evolution of the sweptback wing for efficient flight at supersonic speeds has reached the point where the stability and control problems are being investigated. This situation implies that not only the lift and drag of the wing but also the pitching moment must be considered in relation to the airplane as a whole.

In order to be truly efficient at the design Mach number, the wing should produce the design lift coefficient without creating about the airplane center of gravity a pitching moment that would require a large deflection of the trimming device (with a correspondingly large drag). In addition, it is generally desirable that the spanwise distribution of lift be as nearly elliptical as possible and that any adverse pressure gradients on the wing be small so as to retard separation of the flow. These two conditions are not sufficient to guarantee that the wing drag will be a minimum because at supersonic speeds the drag due to lift is also dependent on the chordwise loading; they are, however, conducive to low wing drag.

The use of wings warped to produce a constant pressure over the surface has been proposed to eliminate the large adverse pressure gradients encountered with the flat wing. For a given plan form, however, a uniform pressure distribution allows no control over the pitching moment. The wing warp necessary to produce certain other pressure distributions has been derived (ref. 1), but these distributions do not lend themselves readily to the control of pitching moment; in fact, the conical nature of the pressure distributions fixes the center of pressure at the center of area for triangular wings.

In the present report, data are presented from which the wing warp necessary to produce a certain type of pressure distribution may be determined. A development is then given in which certain constants appearing in the expression for the pressure distribution are determined by conditions on the lift, pitching moment, and spanwise load distribution. In this manner a method is derived for designing a wing of given plan form, operating at a given supersonic Mach number, to have a specified lift coefficient, a specified center of pressure, and a nearly elliptical spanwise load distribution. Although the pressure gradients are not controlled directly in the method, the type of pressure distribution used insures that for most reasonable design conditions the gradients will not be excessive. There is no reason to believe that a configuration using a self-trimming device designed by this method will necessarily have a lower drag than will a similar configuration using a flat wing and a deflected trimming device. The possibility does exist, however, and should probably be investigated.

The method is applicable to a wide class of wing plan forms shown in figure 1; the principal requirement is that the leading edge must be subsonic and the trailing edge must be supersonic. The presentation is made in a form suitable for engineering use, and a table and computational form are provided so that the application of the method is reduced to routine computation.

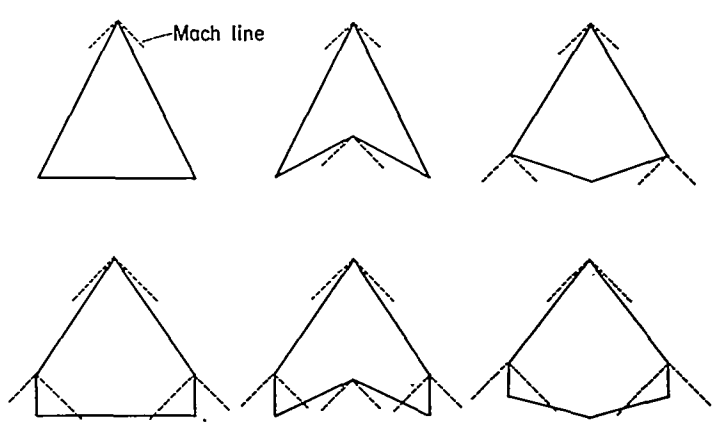

Figure 1.—Plan forms to which the method is applicable.

[1] Supersedes recently declassified NACA RM L51F03, 1951.

SYMBOLS

$A_0 \equiv \frac{\sigma(1-\lambda)}{(1-k)[1-\sigma(1-\lambda)]}$

$\beta \equiv \sqrt{M^2-1}$

c local chord

c_r root chord

$\bar{c}$ mean aerodynamic chord, $\frac{2}{S}\int_0^s c^2 dy = \frac{2(1+\lambda+\lambda^2)}{3(1+\lambda)} c_r$

C_D drag coefficient, $\frac{\text{Drag}}{qS}$

c_l local lift coefficient, $\frac{\text{Lift on chordwise strip } dy \text{ in width}}{qc}$

C_L lift coefficient, $\frac{\text{Lift}}{qS}$

C_m pitching-moment coefficient, positive when pitching moment tends to move wing apex up, $\frac{\text{Pitching moment}}{qS\bar{c}}$

$k \equiv \frac{m}{m_1}$

λ taper ratio, $\frac{\text{Tip chord}}{\text{Root chord}}$

m cotangent of sweepback angle of leading edge (see fig. 2)

m_1 cotangent of sweepback angle of trailing edge (see fig. 2)

M free-stream Mach number

$n \equiv \beta m$ (see fig. 3)

p_L static pressure on lower surface of wing

p_U static pressure on upper surface of wing

P lifting-pressure coefficient, $\frac{p_L - p_U}{q}$

q free-stream dynamic pressure

$r \equiv \frac{y}{mx}$ (see fig. 3)

s wing semispan (see fig. 2)

$\sigma \equiv \frac{|y|}{s}$

S wing area

x,y rectangular coordinates parallel and normal, respectively, to free stream, with origin at wing apex (see fig. 2)

x' distance behind leading edge measured in free-stream direction

x_0 distance of moment axis behind wing apex (see fig. 5)

$\bar{x'}$ distance of moment axis behind leading edge of mean aerodynamic chord (see fig. 5)

z distance perpendicular to xy-plane, positive up

ANALYSIS

GENERAL

A convenient method is derived in reference 2 for finding the wing shape corresponding to a given pressure distribution. In the present report, the lifting-pressure distribution over the wing is taken to be of the form

$$P = C_1' + C_2'x + C_3'|y| + C_4'y^2 \quad (1)$$

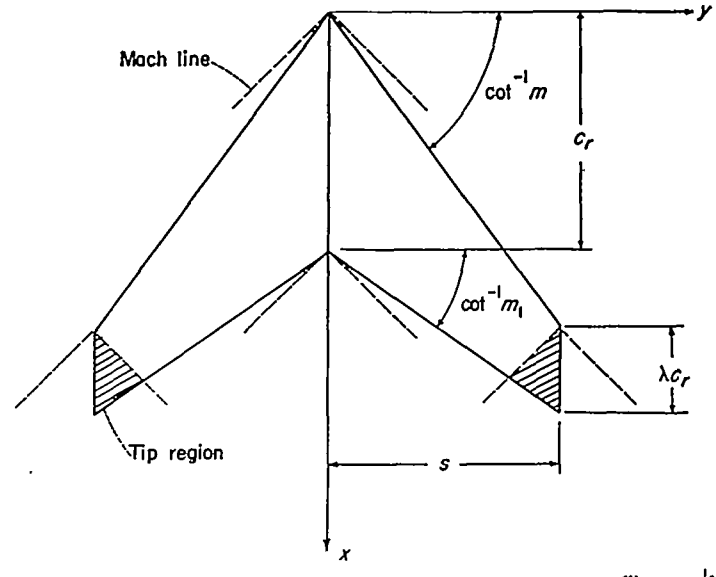

FIGURE 2.—Axis system for pressure distribution. $k \equiv \frac{m}{m_1}$; $\sigma \equiv \frac{|y|}{s}$.

where the axis system is that shown in figure 2, and C_1', C_2', C_3', and C_4' are as yet arbitrary constants. Other terms could have been included in the series but the terms shown gave acceptable results without requiring undue labor. For convenience, the coefficients of the series may be replaced by others similar in nature such that the lifting-pressure distribution can be expressed by the following equation:

$$\frac{P}{C_L} = \frac{C_1}{C_L} + \frac{1-k}{1-\lambda}\frac{C_2}{C_L}\frac{x}{c_r} + \frac{C_3}{C_L}\sigma + \frac{C_4}{C_L}\sigma^2 \quad (2)$$

For purposes of calculation, the wing is assumed to have no thickness so that the shape derived is actually the mean surface of the wing. Within the assumptions of the linearized theory, an arbitrary thickness distribution, symmetrical above and below the mean surface, can then be added with no effect on the lift and pitching moment.

Suitable integrations of the pressure distribution over the plan form may be performed to obtain equations for the lift coefficient, the pitching-moment coefficient, and the spanwise load distribution. One condition may then be imposed on the lift, one on the pitching moment, and two on the spanwise load distribution. This procedure results in four linear equations in the four unknowns C_1/C_L, C_2/C_L, C_3/C_L, and C_4/C_L. The values for these constants may then be substituted into equation (2), and the shape of the wing (that is, the warp) necessary to produce this pressure distribution can be found by the method of reference 2.

The foregoing material has described the method in general terms. In the following sections more detailed descriptions are given: First, of the procedure used to find the warp corresponding to each component of the pressure distribution; second, of the method used to determine the constants for the case of plan forms having pointed tips; and last, of the corresponding procedure for plan forms having finite tip chords. Although the determination of the constants is in principle the same for both types of plan forms, certain simplifications occurring for the pointed-tip case make not only the actual numerical work of determining the constants but also the exposition of the procedure simpler for this case.

WARP

The warps or wing shapes necessary to produce the several components of the pressure distribution given in equation (2) are first found separately as functions of the four constants C_1/C_L, C_2/C_L, C_3/C_L, and C_4/C_L. Later, after numerical values of the constants have been determined by the conditions imposed on the lift, pitching moment, and spanwise load distribution, the separate shapes are superimposed to form the final warped wing.

The general idea in finding each wing shape is first to determine the slope of the wing surface $\left(\frac{dz}{dx}\right)_{z=0}$ associated with the pressure distribution under consideration and then to integrate this slope in the x-direction to get the z-ordinate at any point (the direction of z is taken mutually perpendicular to x and y, positive upwards). Of the available methods for finding the wing slope corresponding to a given pressure distribution, that presented in reference 2 was chosen for the particular problem. The principal advantage of this method is that it eliminates the need for considering z in the integrations involved and so simplifies the integrations.

The slope of the wing surface corresponding to each term of equation (2) is found by application of equations (8) and (17) of reference 2. The wing shape as a displacement from the $z=0$ plane is then found by integrating the slope in the x-direction; thus,

$$z=\int_{\beta y}^{x}\left(\frac{dz}{dx}\right)_{z=0}dx \tag{3}$$

The following equations result for the wing shapes corresponding to the four components of the pressure:

$$z_1=\frac{C_L\left(\frac{C_1}{C_L}\right)}{m}xR_1\equiv\frac{C_L\left(\frac{C_1}{C_L}\right)}{m}x\frac{1}{4\pi}\left[2\sqrt{1-n^2r^2}-2\cosh^{-1}\left|\frac{1}{nr}\right|+\sqrt{1-n^2}(1+r)\cosh^{-1}\left|\frac{1+n^2r}{n(1+r)}\right|+\sqrt{1-n^2}(1-r)\cosh^{-1}\left|\frac{1-n^2r}{n(1-r)}\right|\right] \tag{4a}$$

$$z_2=\frac{C_L\left(\frac{C_2}{C_L}\right)}{s}x^2R_2\equiv-\frac{C_L\left(\frac{C_2}{C_L}\right)}{s}x^2\frac{1}{4\pi}\left\{\sqrt{1-n^2r^2}-2r^2\cosh^{-1}\left|\frac{1}{nr}\right|+\frac{1}{\sqrt{1-n^2}}\left[\frac{n^2(1-r^2)}{2}+r+r^2\right]\cosh^{-1}\left|\frac{1+n^2r}{n(1+r)}\right|+\frac{1}{\sqrt{1-n^2}}\left[\frac{n^2(1-r^2)}{2}-r+r^2\right]\cosh^{-1}\left|\frac{1-n^2r}{n(1-r)}\right|\right\} \tag{4b}$$

$$z_3=\frac{C_L\left(\frac{C_3}{C_L}\right)}{s}x^3R_3\equiv-\frac{C_L\left(\frac{C_3}{C_L}\right)}{s}x^2\frac{1}{4\pi}\left[\frac{5}{2}\sqrt{1-n^2r^2}-\left(1+3r^2-\frac{1}{2}n^2r^2\right)\cosh^{-1}\left|\frac{1}{nr}\right|+\frac{(1+r)^2+2(1-n^2)(r+r^2)}{2\sqrt{1-n^2}}\cosh^{-1}\left|\frac{1+n^2r}{n(1+r)}\right|+\frac{(1-r)^2-2(1-n^2)(r-r^2)}{2\sqrt{1-n^2}}\cosh^{-1}\left|\frac{1-n^2r}{n(1-r)}\right|\right] \tag{4c}$$

$$z_4=\frac{mC_L\left(\frac{C_4}{C_L}\right)}{s^2}x^3R_4\equiv\frac{mC_L\left(\frac{C_4}{C_L}\right)}{s^2}x^3\frac{1}{4\pi}\left\{\frac{(1-n^2r^2)^{3/2}}{3(1-n^2)}+\frac{12-10n^2}{3n^2(1-n^2)}n^2r^2\sqrt{1-n^2r^2}-6r^2\cosh^{-1}\left|\frac{1}{nr}\right|+\frac{1}{(1-n^2)^{3/2}}\left[\frac{6-9n^2+2n^4}{2}(r^2+r^3)+\frac{2-3n^2}{2}(r-r^3)-\frac{n^2}{6}(1+r^3)\right]\cosh^{-1}\left|\frac{1+n^2r}{n(1+r)}\right|+\frac{1}{(1-n^2)^{3/2}}\left[\frac{6-9n^2+2n^4}{2}(r^2-r^3)-\frac{2-3n^2}{2}(r-r^3)-\frac{n^2}{6}(1-r^3)\right]\cosh^{-1}\left|\frac{1-n^2r}{n(1-r)}\right|\right\} \tag{4d}$$

The significance of the quantities r and n is most clearly seen by reference to figure 3. Calculations have been made of the quantities R_1, R_2, R_3, and R_4, which are in a certain sense the conical parts of the wing shapes, and the results are presented in figure 4 and table I. The figure is intended to be merely illustrative; the results in the table should be used for actual calculations. A study of the figure provides a qualitative idea of the various wing shapes. One interesting fact to notice is that no infinities occur at the center line ($r=0$) for the cases in which the pressure is proportional to x and to y^2. (Compare with the shapes derived in ref. 1.)

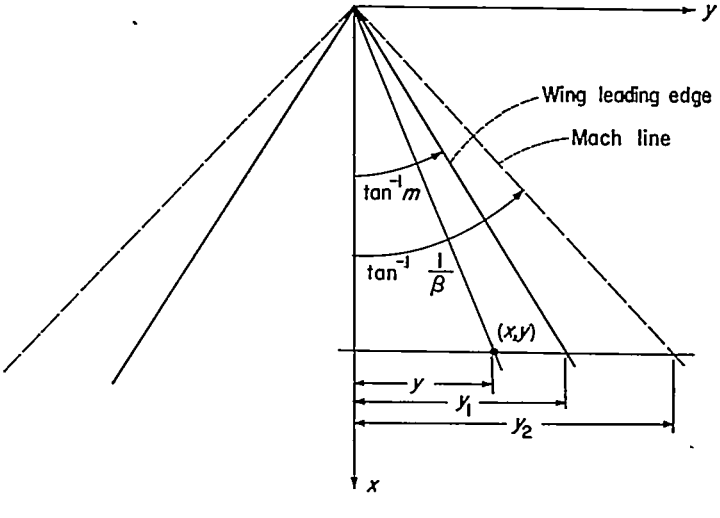

FIGURE 3.—Definitions of r and n: $r\equiv\frac{y}{y_1}=\frac{y}{mx}$; $n\equiv\frac{y_1}{y_2}=\beta m$.

EVALUATION OF CONSTANTS FOR POINTED-TIP WINGS ($\lambda=0$)

The pressure distribution given by equation (2) is integrated over the plan form to obtain an expression for the lift of the wing. If the limits shown in figure 5 are used, the following equation expresses the value of the lift:

$$\frac{\text{Lift}}{q}=2C_L\int_0^s dy\int_{y/m}^{c_r+\frac{ky}{m}}\frac{P}{C_L}dx \tag{5}$$

If the indicated operations are carried out and the lift coefficient is formed, the following equation results:

$$1=\frac{C_1}{C_L}+\frac{2-k}{3}\frac{C_2}{C_L}+\frac{1}{3}\frac{C_3}{C_L}+\frac{1}{6}\frac{C_4}{C_L} \tag{6}$$

The pitching moment about an axis a distance x_0 behind the wing apex may also be found by the following equation:

$$\frac{M}{q}=-2C_L\int_0^s dy\int_{y/m}^{c_r+\frac{ky}{m}}(x-x_0)\frac{P}{C_L}\,dx \tag{7}$$

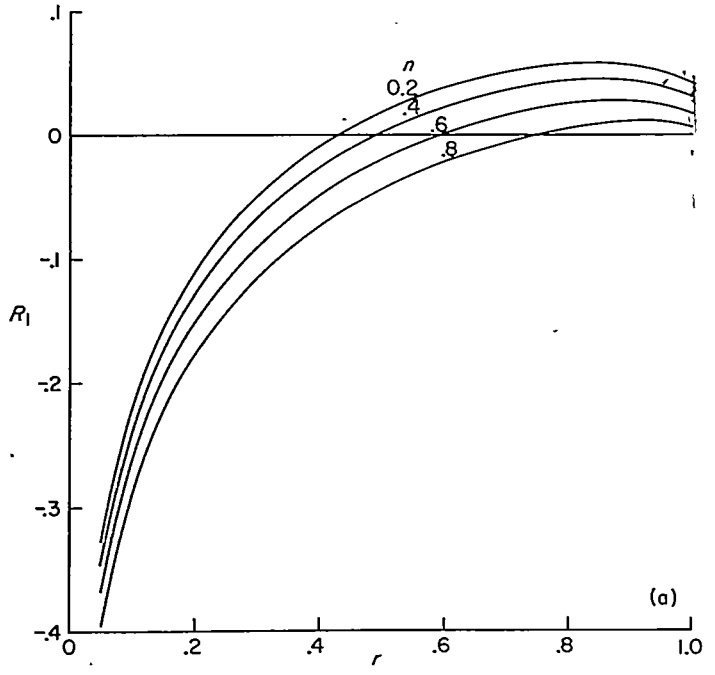

(a) R_1.

FIGURE 4.—Values of R_1, R_2, R_3, and R_4.

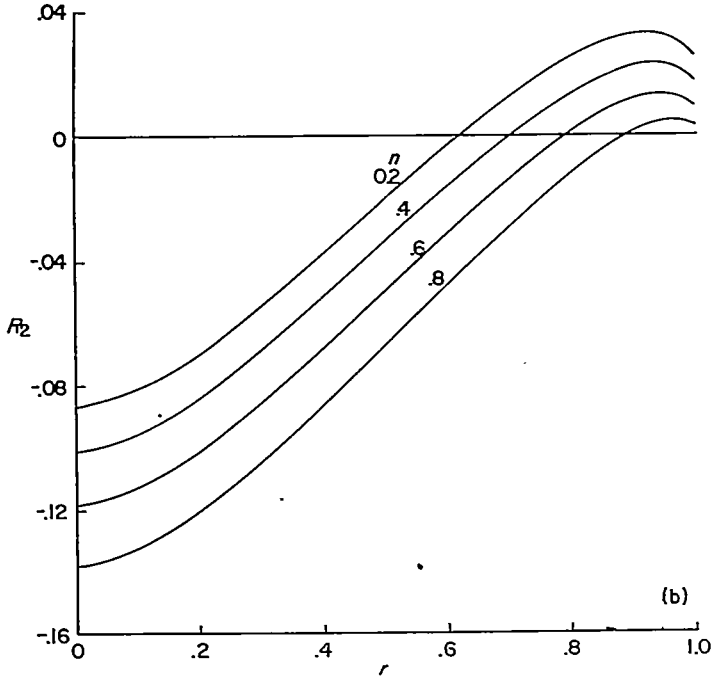

(b) R_2.

FIGURE 4.—Continued.

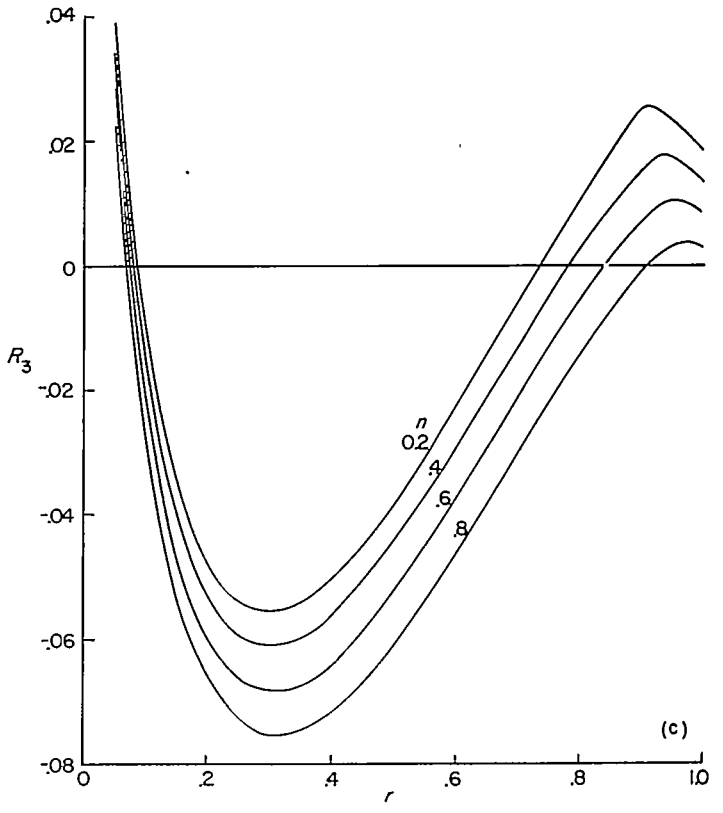

(c) R_3.

FIGURE 4.—Continued.

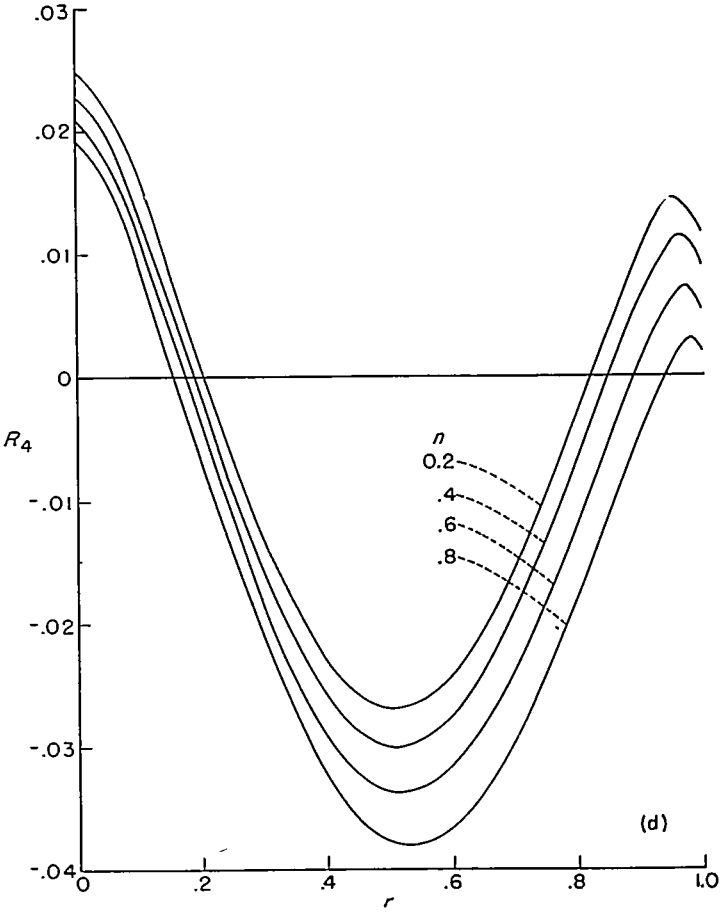

(d) R_4.

FIGURE 4.—Concluded.

TABLE I.—VALUES OF R_1, R_2, R_3, R_4

r	n = 0.1				n = 0.2				n = 0.3			
	R_1	R_2	R_3	R_4	R_1	R_2	R_3	R_4	R_1	R_2	R_3	R_4
0	−∞	−0.0820	∞	0.0260	−∞	−0.0870	∞	0.0250	−∞	−0.0936	∞	0.0240
.02	−0.4663	−.0817	0.1119	.0253	−0.4275	−.0866	0.1099	.0244	−0.4810	−.4810	0.1075	.0233
.04	−.3561	−.0890	.0579	.0238	−.3623	−.0860	.0559	.0228	−.3707	−.0925	.0535	.0218
.06	−.2917	−.0798	.0274	.0217	−.2979	−.0848	.0254	.0208	−.3064	−.0915	.0230	.0197
.08	−.2463	−.0784	.0068	.0193	−.2523	−.0834	.0047	.0183	−.2608	−.0900	.0023	.0173
.10	−.2109	−.0767	−.0084	.0166	−.2171	−.0818	−.0104	.0161	−.2255	−.0884	−.0129	.0145
.12	−.1825	−.0749	−.0198	.0137	−.1884	−.0799	−.0219	.0127	−.1969	−.0865	−.0244	.0116
.14	−.1581	−.0728	−.0289	.0106	−.1643	−.0778	−.0309	.0097	−.1729	−.0844	−.0334	.0086
.16	−.1372	−.0704	−.0359	.0076	−.1435	−.0755	−.0379	.0066	−.1519	−.0820	−.0404	.0055
.18	−.1191	−.0680	−.0413	.0045	−.1248	−.0730	−.0436	.0035	−.1337	−.0796	−.0458	.0024
.20	−.1030	−.0654	−.0454	.0014	−.1091	−.0704	−.0475	.0004	−.1175	−.0769	−.0501	−.0007
.24	−.0770	−.0597	−.0509	−.0046	−.0815	−.0648	−.0530	−.0056	−.0899	−.0713	−.0556	−.0067
.28	−.0525	−.0538	−.0533	−.0100	−.0586	−.0587	−.0564	−.0111	−.0669	−.0652	−.0580	−.0123
.32	−.0332	−.0474	−.0533	−.0149	−.0393	−.0523	−.0555	−.0159	−.0476	−.0587	−.0582	−.0172
.36	−.0167	−.0407	−.0516	−.0189	−.0228	−.0456	−.0538	−.0200	−.0310	−.0520	−.0566	−.0213
.40	−.0029	−.0340	−.0485	−.0220	−.0085	−.0387	−.0507	−.0233	−.0166	−.0450	−.0535	−.0243
.44	.0093	−.0268	−.0442	−.0243	.0039	−.0317	−.0464	−.0254	−.0042	−.0379	−.0493	−.0268
.48	.0205	−.0198	−.0390	−.0255	.0146	−.0246	−.0413	−.0266	.0067	−.0308	−.0442	−.0281
.52	.0298	−.0128	−.0331	−.0256	.0239	−.0181	−.0354	−.0268	.0160	−.0236	−.0383	−.0284
.56	.0376	−.0059	−.0268	−.0247	.0320	−.0106	−.0263	−.0260	.0242	−.0166	−.0321	−.0276
.60	.0445	.0009	−.0201	−.0228	.0388	−.0038	−.0224	−.0241	.0311	−.0097	−.0255	−.0258
.65	.0515	.0089	−.0115	−.0192	.0458	.0044	−.0139	−.0205	.0383	−.0014	−.0169	−.0222
.70	.0568	.0164	−.0029	−.0142	.0511	.0120	−.0053	−.0156	.0438	.0064	−.0084	−.0173
.75	.0605	.0232	.0053	−.0082	.0550	.0188	.0030	−.0096	.0479	.0134	−.0001	−.0114
.80	.0625	.0289	.0128	−.0015	.0573	.0247	.0105	−.0029	.0503	.0194	.0074	−.0047
.82	.0629	.0308	.0156	.0013	.0577	.0267	.0132	−.0002	.0508	.0215	.0102	−.0020
.84	.0630	.0325	.0180	.0040	.0578	.0284	.0157	.0026	.0510	.0234	.0127	.0007
.86	.0628	.0340	.0203	.0067	.0575	.0308	.0179	.0052	.0509	.0249	.0150	.0034
.88	.0622	.0351	.0222	.0092	.0571	.0311	.0200	.0078	.0505	.0262	.0170	.0058
.90	.0613	.0360	.0238	.0115	.0563	.0319	.0216	.0101	.0498	.0272	.0187	.0083
.91	.0606	.0361	.0245	.0126	.0557	.0322	.0222	.0112	.0493	.0275	.0194	.0094
.92	.0599	.0362	.0250	.0136	.0550	.0323	.0228	.0122	.0486	.0277	.0199	.0103
.93	.0591	.0361	.0254	.0144	.0542	.0323	.0232	.0130	.0479	.0277	.0203	.0113
.94	.0581	.0360	.0256	.0152	.0532	.0322	.0234	.0138	.0470	.0277	.0206	.0120
.95	.0570	.0356	.0256	.0157	.0521	.0319	.0235	.0144	.0460	.0275	.0208	.0126
.96	.0556	.0351	.0255	.0161	.0507	.0313	.0233	.0146	.0448	.0270	.0207	.0130
.97	.0541	.0343	.0251	.0162	.0494	.0307	.0230	.0148	.0434	.0264	.0203	.0132
.98	.0524	.0331	.0241	.0159	.0476	.0296	.0223	.0146	.0419	.0254	.0197	.0130
.99	.0500	.0316	.0231	.0152	.0454	.0281	.0211	.0140	.0396	.0240	.0186	.0124
1.00	.0466	.0289	.0207	.0133	.0421	.0254	.0187	.0121	.0359	.0214	.0163	.0106

TABLE I.—VALUES OF R_1, R_2, R_3, R_4—Continued

r	n = 0.4				n = 0.5				n = 0.6			
	R_1	R_2	R_3	R_4	R_1	R_2	R_3	R_4	R_1	R_2	R_3	R_4
0	−∞	−0.1013	∞	0.0229	−∞	−0.1098	∞	0.0219	−∞	−0.1189	∞	0.0210
.02	−0.4911	−.1010	0.1049	.0223	−0.5026	−.1095	0.1021	.0212	−0.5153	−.1186	0.0994	.0203
.04	−.3806	−.1003	.0507	.0207	−.3924	−.1087	.0481	.0197	−.4050	−.1178	.0453	.0187
.06	−.3165	−.0991	.0203	.0187	−.3282	−.1076	.0177	.0176	−.3408	−.1167	.0147	.0166
.08	−.2709	−.0977	−.0004	.0162	−.2824	−.1062	−.0032	.0152	−.2950	−.1153	−.0061	.0142
.10	−.2357	−.0960	−.0156	.0135	−.2471	−.1045	−.0184	.0124	−.2597	−.1135	−.0213	.0114
.12	−.2070	−.0941	−.0271	.0105	−.2184	−.1026	−.0300	.0095	−.2310	−.1116	−.0330	.0084
.14	−.1828	−.0920	−.0361	.0075	−.1943	−.1005	−.0390	.0064	−.2067	−.1095	−.0421	.0054
.16	−.1620	−.0897	−.0431	.0044	−.1740	−.0979	−.0456	.0032	−.1859	−.1071	−.0492	.0022
.18	−.1438	−.0872	−.0487	.0012	−.1552	−.0956	−.0516	.0001	−.1676	−.1046	−.0548	−.0010
.20	−.1276	−.0845	−.0529	−.0019	−.1389	−.0929	−.0560	−.0031	−.1514	−.1019	−.0591	−.0042
.24	−.0999	−.0783	−.0585	−.0080	−.1111	−.0872	−.0616	−.0093	−.1235	−.0961	−.0650	−.0104
.28	−.0769	−.0727	−.0610	−.0136	−.0881	−.0809	−.0643	−.0148	−.1003	−.0898	−.0677	−.0161
.32	−.0566	−.0662	−.0613	−.0185	−.0686	−.0743	−.0646	−.0199	−.0807	−.0831	−.0680	−.0213
.36	−.0408	−.0593	−.0597	−.0227	−.0518	−.0674	−.0632	−.0242	−.0638	−.0761	−.0669	−.0256
.40	−.0203	−.0523	−.0567	−.0260	−.0373	−.0603	−.0603	−.0276	−.0491	−.0688	−.0641	−.0292
.44	−.0138	−.0451	−.0526	−.0284	−.0250	−.0529	−.0560	−.0303	−.0363	−.0614	−.0601	−.0318
.48	−.0029	−.0379	−.0476	−.0298	−.0135	−.0456	−.0513	−.0315	−.0250	−.0539	−.0554	−.0333
.52	.0057	−.0306	−.0419	−.0301	−.0038	−.0382	−.0457	−.0319	−.0151	−.0463	−.0498	−.0339
.56	.0149	−.0234	−.0355	−.0294	.0046	−.0309	−.0395	−.0313	−.0065	−.0383	−.0437	−.0334
.60	.0208	−.0171	−.0295	−.0277	.0119	−.0237	−.0330	−.0297	.0019	−.0318	−.0383	−.0318
.65	.0294	−.0079	−.0205	−.0242	.0196	−.0150	−.0246	−.0264	.0090	−.0224	−.0289	−.0288
.70	.0352	.0000	−.0120	−.0194	.0257	−.0068	−.0160	−.0217	.0154	−.0139	−.0204	−.0242
.75	.0395	.0073	−.0038	−.0135	.0303	.0007	−.0078	−.0159	.0204	−.0060	−.0121	−.0186
.80	.0422	.0136	.0038	−.0069	.0333	.0074	−.0001	−.0095	.0240	.0010	−.0044	−.0121
.82	.0428	.0158	.0066	−.0042	.0341	.0097	.0027	−.0067	.0249	.0036	−.0014	−.0095
.84	.0432	.0177	.0092	−.0015	.0347	.0119	.0053	−.0040	.0258	.0058	.0010	−.0065
.86	.0432	.0195	.0115	.0012	.0349	.0137	.0077	−.0012	.0262	.0079	.0037	−.0041
.88	.0431	.0208	.0135	.0039	.0349	.0153	.0098	.0013	.0265	.0097	.0058	−.0013
.90	.0422	.0218	.0154	.0060	.0345	.0165	.0116	.0037	.0263	.0112	.0077	.0010
.91	.0420	.0223	.0160	.0073	.0342	.0170	.0124	.0050	.0262	.0117	.0085	.0024
.92	.0414	.0226	.0166	.0083	.0338	.0174	.0131	.0069	.0259	.0123	.0093	.0034
.93	.0408	.0228	.0171	.0092	.0333	.0177	.0137	.0070	.0255	.0127	.0099	.0044
.94	.0400	.0228	.0175	.0100	.0326	.0179	.0141	.0076	.0251	.0131	.0105	.0053
.95	.0391	.0227	.0176	.0106	.0318	.0178	.0142	.0085	.0244	.0131	.0108	.0059
.96	.0380	.0224	.0176	.0110	.0308	.0176	.0143	.0089	.0237	.0131	.0109	.0066
.97	.0367	.0218	.0173	.0113	.0298	.0172	.0141	.0093	.0228	.0128	.0108	.0071
.98	.0351	.0210	.0168	.0112	.0283	.0165	.0137	.0091	.0216	.0123	.0105	.0072
.99	.0332	.0197	.0158	.0106	.0266	.0154	.0128	.0088	.0200	.0114	.0098	.0068
1.00	.0302	.0173	.0136	.0090	.0238	.0133	.0109	.0071	.0175	.0096	.0081	.0054

TABLE I.—VALUES OF R_1, R_2, R_3, R_4—Concluded

r	n = 0.7				n = 0.8				n = 0.9			
	R_1	R_2	R_3	R_4	R_1	R_2	R_3	R_4	R_1	R_2	R_3	R_4
0	−∞	−0.1284	∞	0.0200	∞	−0.1384	∞	0.0192	−∞	−0.1487	∞	0.0184
.02	−0.5288	−.1282	0.0968	.0194	−0.5431	−.1381	0.0941	.0185	−0.5582	−.1483	0.0911	.0177
.04	−.4185	−.1274	.0425	.0178	−.4329	−.1373	.0397	.0170	−.4479	−.1475	.0369	.0162
.06	−.3541	−.1262	.0119	.0157	−.3685	−.1362	.0090	.0149	−.3835	−.1464	.0062	0140
.08	−.3085	−.1248	−.0090	.0132	−.3228	−.1347	−.0118	.0123	−.3378	−.1449	−.0147	.0115
.10	−.2732	−.1231	−.0242	.0104	−.2876	−.1330	−.0272	.0095	−.3000	−.1432	−.0310	.0087
.12	−.2445	−.1211	−.0359	.0075	−.2587	−.1310	−.0389	.0065	−.2737	−.1411	−.0419	.0050
.14	−.2202	−.1190	−.0451	.0043	−.2345	−.1289	−.0481	.0034	−.2494	−.1389	−.0551	.0025
.16	−.1994	−.1165	−.0522	.0011	−.2136	−.1262	−.0551	.0001	−.2284	−.1365	−.0595	−.0008
.18	−.1812	−.1140	−.0579	−.0021	−.1952	−.1238	−.0611	−.0031	−.2100	−.1339	−.0643	−.0041
.20	−.1647	−.1113	−.0623	−.0053	−.1788	−.1210	−.0656	−.0064	−.1936	−.1310	−.0689	−.0074
.24	−.1368	−.1054	−.0683	−.0116	−.1508	−.1150	−.0717	−.0128	−.1654	−.1250	−.0752	−.0139
.28	−.1135	−.0990	−.0712	−.0174	−.1274	−.1086	−.0748	−.0187	−.1419	−.1184	−.0784	−.0200
.32	−.0937	−.0922	−.0718	−.0227	−.1075	−.1017	−.0756	−.0241	−.1218	−.1114	−.0794	−.0255
.36	−.0767	−.0851	−.0706	−.0272	−.9003	−.0944	−.0746	−.0287	−.1044	−.1040	−.0786	−.0304
.40	−.0618	−.0777	−.0680	−.0309	−.0752	−.0869	−.0721	−.0325	−.0891	−.0963	−.0764	−.0343
.44	−.0488	−.0701	−.0642	−.0336	−.0619	−.0792	−.0686	−.0353	−.0756	−.0884	−.0729	−.0373
.48	−.0374	−.0625	−.0596	−.0353	−.0506	−.0713	−.0637	−.0375	−.0637	−.0804	−.0685	−.0394
.52	−.0273	−.0547	−.0541	−.0360	−.0399	−.0634	−.0587	−.0382	−.0530	−.0722	−.0634	−.0405
.56	−.0183	−.0470	−.0482	−.0357	−.0307	−.0555	−.0529	−.0380	−.0434	−.0641	−.0577	−.0405
.60	−.0105	−.0394	−.0418	−.0343	−.0225	−.0476	−.0466	−.0369	−.0350	−.0560	−.0515	−.0395
.65	−.0022	−.0301	−.0335	−.0313	−.0137	−.0380	−.0383	−.0341	−.0251	−.0458	−.0433	−.0373
.70	.0047	−.0213	−.0250	−.0269	−.0063	−.0287	−.0299	−.0298	−.0175	−.0363	−.0351	−.0329
.75	.0102	−.0130	−.0167	−.0214	−.0002	−.0200	−.0216	−.0244	−.0108	−.0270	−.0266	−.0275
.80	.0144	−.0055	−.0090	−.0150	.0046	−.0120	−.0137	−.0181	−.0052	−.0185	−.0187	−.0213
.82	.0156	−.0028	−.0060	−.0127	.0062	−.0091	−.0108	−.0154	−.0033	−.0153	−.0156	−.0180
.84	.0167	−.0004	−.0034	−.0094	.0075	−.0063	−.0079	−.0124	−.0016	−.0122	−.0125	−.0158
.86	.0174	.0020	−.0007	−.0068	.0086	−.0037	−.0052	−.0099	−.0001	−.0094	−.0101	−.0131
.88	.0180	.0040	.0016	−.0041	.0095	−.0015	−.0028	−.0072	.0013	−.0068	−.0072	−.0101
.90	.0182	.0058	.0036	−.0016	.0101	.0007	−.0004	−.0046	.0022	−.0044	−.0047	−.0076
.91	.0181	.0066	.0046	−.0005	.0103	.0015	.0005	−.0033	.0027	−.0032	−.0035	−.0062
.92	.0180	.0072	.0054	.0007	.0104	.0023	.0014	−.0021	.0031	−.0022	−.0024	−.0049
.93	.0179	.0078	.0061	.0017	.0104	.0031	.0022	−.0011	.0034	−.0013	−.0017	−.0038
.94	.0176	.0082	.0067	.0028	.0104	.0037	.0029	.0000	.0037	−.0004	−.0007	−.0026
.95	.0171	.0085	.0072	.0035	.0103	.0042	.0035	.0009	.0038	.0002	−.0001	−.0017
.96	.0166	.0087	.0075	.0041	.0099	.0046	.0040	.0017	.0039	.0009	.0007	−.0000
.97	.0158	.0086	.0076	.0046	.0095	.0048	.0044	.0023	.0038	.0013	.0011	.0001
.98	.0150	.0083	.0074	.0049	.0089	.0048	.0043	.0028	.0036	.0017	.0016	.0007
.99	.0137	.0077	.0069	.0049	.0080	.0045	.0042	.0027	.0033	.0017	.0016	.0011
1.00	.0117	.0062	.0055	.0037	.0055	.0036	.0031	.0021	.0024	.0010	.0009	.0007

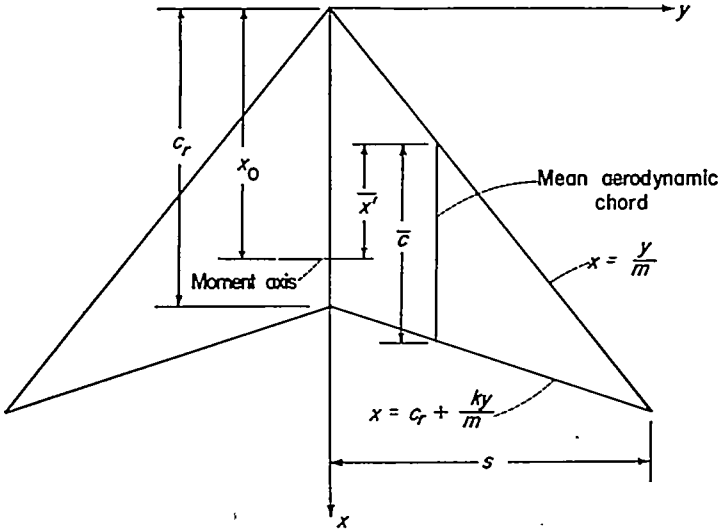

FIGURE 5.—Limits of integration for pointed-tip wing.

After the pitching-moment coefficient is formed, the following equation is obtained:

$$\frac{C_m}{C_L}=\left[\frac{3}{2}\frac{x_0}{c_r}-\frac{2-k}{2(1-k)}\right]\frac{C_1}{C_L}+\left[\frac{2-k}{2}\frac{x_0}{c_r}-\frac{3-3k+k^2}{4(1-k)}\right]\frac{C_2}{C_L}+$$
$$\left[\frac{1}{2}\frac{x_0}{c_r}-\frac{3-k}{8(1-k)}\right]\frac{C_3}{C_L}+\left[\frac{1}{4}\frac{x_0}{c_r}-\frac{4-k}{20(1-k)}\right]\frac{C_4}{C_L} \tag{8}$$

The spanwise load distribution is found from the following integration:

$$\frac{cc_l}{c_rC_L}=\frac{1}{c_r}\int_{y/m}^{c_r+\frac{ky}{m}}\frac{P}{C_L}\,dx$$

where c is the local chord and c_l is the local lift coefficient. The integration has already been made in finding the lift. The following equation results:

$$\frac{cc_l}{c_rC_L}=\left(\frac{C_1}{C_L}+\frac{1-k}{2}\frac{C_2}{C_L}\right)-\left(\frac{C_1}{C_L}-k\frac{C_2}{C_L}-\frac{C_3}{C_L}\right)\sigma-$$
$$\left(\frac{1+k}{2}\frac{C_2}{C_L}+\frac{C_3}{C_L}-\frac{C_4}{C_L}\right)\sigma^2-\frac{C_4}{C_L}\sigma^3 \tag{9}$$

For purposes of reference, the spanwise load distribution if elliptical would be given by the following equation:

$$\frac{cc_l}{c_rC_L}=\frac{2(1+\lambda)}{\pi}\sqrt{1-\sigma^2} \tag{10}$$

where $\lambda=0$ for the pointed-tip case. Equations (6), (8), and (9) are now used to find values for C_1/C_L, C_2/C_L, C_3/C_L, and C_4/C_L. The following conditions are first applied to equation (9):

$$\left.\begin{aligned}\left(\frac{cc_l}{c_rC_L}\right)_{\sigma=0}&=\frac{2(1+\lambda)}{\pi}\quad\text{(value for ellipse)}\\ \left[\frac{d\left(\frac{cc_l}{c_rC_L}\right)}{d\sigma}\right]_{\sigma=0}&=0\quad\text{(value for ellipse)}\end{aligned}\right\} \tag{11}$$

where again $\lambda=0$ for the pointed-tip case. These conditions are not quite arbitrary but were chosen after trial of a number of possibilities. The selection of these particular conditions not only made possible a solution for the four unknowns but also resulted in a single equation for the

spanwise load distribution which was a fair approximation to an ellipse. (The degree of the approximation is shown subsequently.)

The solution for the constants may now be made. Substitution of equations (11) into equation (9) gives the following values for C_1/C_L and C_2/C_L:

$$\frac{C_1}{C_L}=\frac{4k}{(1+k)\pi}+\frac{1-k}{1+k}\frac{C_3}{C_L}$$

$$\frac{C_2}{C_L}=\frac{4}{(1+k)\pi}-\frac{2}{1+k}\frac{C_3}{C_L}$$

These values are substituted into equation (6) and the following solution for C_4/C_L is got:

$$\frac{C_4}{C_L}=6-\frac{16}{\pi}$$

The values of C_1/C_L, C_2/C_L, and C_4/C_L are substituted into equation (8) and the left-hand side is set equal to zero to arrive at the solution for C_3/C_L. The solutions are collected in the following equations:

$$\left.\begin{aligned}
&\frac{C_4}{C_L}=6-\frac{16}{\pi}\\
&\frac{C_3}{C_L}=\frac{8(1+k)}{1-k}\left[\frac{3(4-k)}{10(1-k)}-\frac{1+7k+k^2}{5\pi(1-k^2)}-\frac{3}{2}\frac{x_0}{c_r}\right]\\
\text{or}\quad&\frac{C_3}{C_L}=\frac{8(1+k)}{1-k}\left[\frac{7-3k}{10(1-k)}-\frac{1+7k+k^2}{5\pi(1-k^2)}-\frac{\bar{x}'}{\bar{c}}\right]\\
&\frac{C_2}{C_L}=\frac{4}{(1+k)\pi}-\frac{2}{1+k}\frac{C_3}{C_L}\\
&\frac{C_1}{C_L}=\frac{4k}{(1+k)\pi}+\frac{1-k}{1+k}\frac{C_3}{C_L}
\end{aligned}\right\}\qquad(12)$$

The two forms for C_3/C_L are given because in some cases the center of pressure is located more conveniently with respect to the mean aerodynamic chord $\bar{c}$. The geometrical relation between x_0 and $\bar{x}'$ is indicated in figure 5; the analytical relation is

$$\frac{x_0}{c_r}=\frac{2}{3}\frac{\bar{x}'}{\bar{c}}+\frac{1}{3(1-k)}\qquad(13)$$

For $k=0$ (triangular wing), equations (12) simplify to the following equations:

$$\left.\begin{aligned}
&\frac{C_4}{C_L}=6-\frac{16}{\pi}\\
&\frac{C_3}{C_L}=8\left(\frac{6}{5}-\frac{1}{5\pi}-\frac{3}{2}\frac{x_0}{c_r}\right)\\
\text{or}\quad&\frac{C_3}{C_L}=8\left(\frac{7}{10}-\frac{1}{5\pi}-\frac{\bar{x}'}{\bar{c}}\right)\\
&\frac{C_2}{C_L}=\frac{4}{\pi}-2\frac{C_3}{C_L}\\
&\frac{C_1}{C_L}=\frac{C_3}{C_L}
\end{aligned}\right\}\qquad(14)$$

When equations (12) are substituted into equation (9), the following equation for the spanwise load distribution is obtained:

$$\frac{cc_l}{c_rC_L}=\frac{2}{\pi}+\left(6-\frac{18}{\pi}\right)\sigma^2-\left(6-\frac{16}{\pi}\right)\sigma^3\qquad(15)$$

This equation is uniformly valid for all pointed-tip wings, independent of the lift, center of pressure, Mach number, and relative sweeps of the leading and trailing edges. The load distribution given by equation (15) is compared with the elliptical distribution of equation (10) in figure 6. As a matter of incidental interest, the spanwise center of load on one wing panel is located 0.409 semispan outboard of the wing center line for the load represented by equation (15) as compared with a corresponding value of 0.424 for the elliptical load.

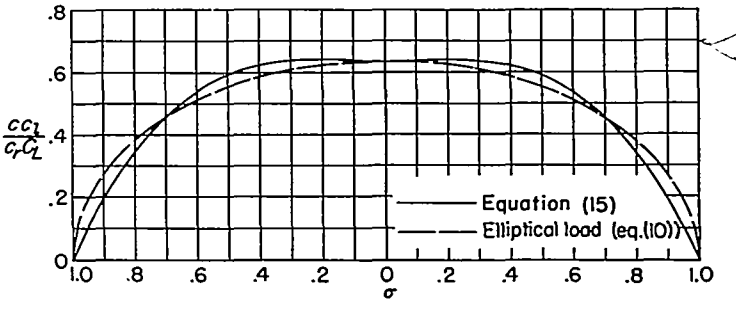

FIGURE 6.—Spanwise load distribution for pointed-tip wings compared with elliptical load distribution.

EVALUATION OF CONSTANTS FOR WINGS WITH FINITE TAPER

The problem of wings with finite taper can be approached in two ways. The more obvious method is to assume that the pressure distribution defined by equation (2) applies over the entire wing surface and to calculate the required warp. (A separate calculation for the warp in the tip region, which is shown shaded in fig. 2, is required, but this calculation is not impossible to make.) The disadvantage of this procedure is that at the tip the required wing slope takes on very large values (theoretically infinite). A more practical approach, and the one adopted in this report, is to relax the condition on the pressure in the tip region. For a flat lifting wing with subsonic leading edges, the average pressure in the tip region is known to be close to zero (refs. 3 and 4). It is not entirely illogical to suppose that for a slightly warped wing the pressure in the tip will also be very small. If for the warped wing the pressure in the tip were taken to be exactly zero, the equations for the lift, pitching moment, and so forth would be derived by first integrating the pressure distribution defined by equation (2) over the entire wing, including the tip region, after which the integral of the same pressure over the tip region would be subtracted. In order to keep the equations within reasonable limits, a constant pressure was instead subtracted from the tip region. The value of this pressure was taken to be the value given by equation (2) at the middle of the tip chord; namely,

$$\frac{P}{C_L}=\frac{C_1}{C_L}+\left[1+\frac{\lambda(1-k)}{2(1-\lambda)}\right]\frac{C_2}{C_L}+\frac{C_3}{C_L}+\frac{C_4}{C_L}\qquad(16)$$

After the foregoing assumption has been made, the determination of the four constants proceeds very similarly to that for the pointed-tip wing: The pressure distribution is integrated to obtain equations for the lift, pitching moment, and spanwise load distribution; two conditions are set on the spanwise load distribution, and the resulting two equations are solved together with the equations for the lift and the pitching moment to give values for the constants C_1/C_L, C_2/C_L, C_3/C_L, and C_4/C_L. The procedure just indicated is now given.

The lift equation, corresponding to equation (6) for the pointed-tip wing, is

$$1=(1-A)\frac{C_1}{C_L}+\left[\frac{2-k}{3(1-\lambda)}-\frac{\lambda^2(1+k)}{3(1-\lambda^2)}-\frac{2-\lambda(1+k)}{2(1-\lambda)}A\right]\frac{C_2}{C_L}+\left[\frac{1+2\lambda}{3(1+\lambda)}-A\right]\frac{C_3}{C_L}+\left[\frac{1+3\lambda}{6(1+\lambda)}-A\right]\frac{C_4}{C_L} \tag{17}$$

where

$$A\equiv\frac{\lambda^2(1-k)}{(k+n)(1-\lambda^2)} \tag{18}$$

In this equation, all the terms containing A arise from integration of the pressure over the tip region, whereas the remainder of the terms represent the integration of equation (2) over the whole wing area. If λ is set equal to zero, the equation reduces to the form given in equation (6).

The pitching-moment equation, corresponding to equation (8) for the pointed-tip wing, is

$$(1+\lambda+\lambda^2)\frac{C_m}{C_L}=\left\{\left[\frac{3(1+\lambda)}{2}-B\right]\frac{x_0}{c_r}-\left[\frac{3(1-k\lambda)}{2(1-k)}-\frac{(1+k)(1-\lambda)^2}{2(1-k)}-C\right]\right\}\frac{C_1}{C_L}+\left(\left\{\frac{3(1-k\lambda)}{2(1-\lambda)}-\frac{(1+k)(1-\lambda)}{2}-\left[\frac{\lambda(1-k)+2(1-\lambda)}{2(1-\lambda)}\right]B\right\}\frac{x_0}{c_r}-\left\{\frac{1-k}{1-\lambda}+\frac{3k}{2}+\frac{k^2(1-\lambda)}{1-k}-\frac{(1+k+k^2)(1-\lambda)^2}{4(1-k)}-\left[\frac{\lambda(1-k)+2(1-\lambda)}{2(1-\lambda)}\right]C\right\}\right)\frac{C_2}{C_L}+\left\{\left(\frac{1+2\lambda}{2}-B\right)\frac{x_0}{c_r}-\left[\frac{3}{4}+\frac{k(1-\lambda)}{1-k}-\frac{3(1+k)(1-\lambda)^2}{8(1-k)}-C\right]\right\}\frac{C_3}{C_L}+\left\{\left(\frac{1+3\lambda}{4}-B\right)\frac{x_0}{c_r}-\left[\frac{1}{2}+\frac{3k(1-\lambda)}{8(1-k)}-\frac{3(1+k)(1-\lambda)^2}{10(1-k)}-C\right]\right\}\frac{C_4}{C_L} \tag{19}$$

where

$$\left.\begin{aligned}B&\equiv\frac{3\lambda^2(1-k)}{2(k+n)(1-\lambda)}\\ C&\equiv\frac{3\lambda^2}{2(k+n)}+\frac{\lambda^3(2n+k)(1-k)}{2(k+n)^2(1-\lambda)}\end{aligned}\right\} \tag{20}$$

The remarks following equation (17), with A replaced by B and C and with equation (6) replaced by equation (8), also apply to equation (19).

Because of the existence of a tip region for the wing of finite taper, the spanwise load distribution must be described by two equations, one applicable from the center line out to the beginning of the tip region and the other applicable over the remainder of the span:

For $0\leqq\sigma\leqq 1-\frac{\lambda(1-k)}{(k+n)(1-\lambda)}$,

$$\frac{cc_l}{c_rC_L}=\left(\frac{C_1}{C_L}+\frac{1-k}{2(1-\lambda)}\frac{C_2}{C_L}\right)-\left[(1-\lambda)\frac{C_1}{C_L}-k\frac{C_2}{C_L}-\frac{C_3}{C_L}\right]\sigma-\left[\frac{(1+k)(1-\lambda)}{2}\frac{C_2}{C_L}+(1-\lambda)\frac{C_3}{C_L}\oplus\frac{C_4}{C_L}\right]\sigma^2-(1-\lambda)\frac{C_4}{C_L}\sigma^3 \tag{21a}$$

For $1-\frac{\lambda(1-k)}{(k+n)(1-\lambda)}\leqq\sigma\leqq 1$,

$$\frac{cc_l}{c_rC_L}=\left\{\frac{(1+n)(1-\lambda)}{1-k}\frac{C_1}{C_L}+\frac{(1-k)^2-[2-\lambda(1+k)][\lambda(1+n)-(k+n)]}{2(1-k)(1-\lambda)}\frac{C_2}{C_L}-\left[\frac{\lambda(1+n)-(k+n)}{1-k}\right]\left(\frac{C_3}{C_L}+\frac{C_4}{C_L}\right)\right\}-\left\{\frac{(1+n)(1-\lambda)}{1-k}\frac{C_1}{C_L}-\frac{(1-\lambda)[2k(1-k)-2(k+n)+\lambda(1+k)(k+n)]}{2(1-k)(1-\lambda)}\frac{C_2}{C_L}-\frac{(1-k)-(1-\lambda)(k+n)}{1-k}\frac{C_3}{C_L}+\frac{(1-\lambda)(k+n)}{1-k}\frac{C_4}{C_L}\right\}\sigma-\left[\frac{(1+k)(1-\lambda)}{2}\frac{C_2}{C_L}+(1-\lambda)\frac{C_3}{C_L}-\frac{C_4}{C_L}\right]\sigma^2-(1-\lambda)\frac{C_4}{C_L}\sigma^3 \tag{21b}$$

The conditions given in equations (11) are now applied to equation (21a) to obtain the following relations:

$$\frac{C_1}{C_L}=\frac{4k(1+\lambda)}{(1+k)\pi}+\frac{1-k}{(1-\lambda)(1+k)}\frac{C_3}{C_L} \tag{22}$$

$$\frac{C_2}{C_L}=\frac{4(1-\lambda^2)}{(1+k)\pi}-\frac{2}{1+k}\frac{C_3}{C_L} \tag{23}$$

These values of C_1/C_L and C_2/C_L are substituted into equation (17) and equation (19). The center of pressure is fixed at x_0 by putting C_m equal to zero in equation (19) and the following equations for C_3/C_L and C_4/C_L are obtained:

$$\frac{C_4}{C_L}=\frac{6(1+\lambda)}{(1+3\lambda)-6(1+\lambda)A}\left[1-\frac{8(1+\lambda)-4\lambda^2}{3\pi}+\frac{(4-2\lambda)(1+\lambda)}{\pi}A\right] \tag{24}$$

$$\frac{(1-k)(1+\lambda+\lambda^2+\lambda^3)}{8(1-\lambda)(1+k)}\frac{C_3}{C_L}+\left\{\left(\frac{1+3\lambda}{4}-B\right)\frac{x_0}{c_r}-\left[\frac{1}{2}+\frac{3k(1-\lambda)}{4(1-k)}-\frac{3(1+k)(1-\lambda)^2}{10(1-k)}-C\right]\right\}\frac{C_4}{C_L}$$

$$=-\frac{2(1+\lambda)}{(1+k)\pi}\left\{[3(1+k)-(1+k)(1-\lambda)^2-(2-\lambda)(1+k)B]\frac{x_0}{c_r}-\right.$$

$$\left.\left[\frac{(3+k-k^2)(1+\lambda)-(3+5k+k^2)\lambda^2+(1+k+k^2)\lambda^3}{2(1-k)}-(2-\lambda)(1+k)C\right]\right\} \tag{25}$$

where A, B, and C are defined in equations (18) and (20).

Equations (24) and (25) can be solved for C_4/C_L and C_3/C_L, after which C_1/C_L and C_2/C_L can be found from equations (22) and (23). This calculation is best done with the numerical values for λ, k, n, and x_0/c_r for the particular wing under consideration. The procedure is illustrated by an example in a subsequent section entitled "Numerical Examples." The relation between x_0/c_r and $\overline{x'}/\overline{c}$ corresponding to equation (13) for the pointed-tip wing is

$$\frac{x_0}{c_r}=\frac{2(1+\lambda+\lambda^2)}{3(1+\lambda)}\frac{\overline{x'}}{\overline{c}}+\frac{1+\lambda-2\lambda^2}{3(1+\lambda)(1-k)} \tag{26}$$

The spanwise load distribution corresponding to equation (15) for the pointed-tip wing can be obtained by substituting equations (22) and (23) into equations (21a) and (21b). The substitution into equation (21b) produces only added complexity, and the result is not given herein. The substitution into equation (21a), however, gives the following simplified equations for $0\leqq\sigma\leqq 1-\frac{\lambda(1-k)}{(k+n)(1-\lambda)}$:

$$\frac{cc_l}{c_rC_L}=\frac{2(1+\lambda)}{\pi}-\left[\frac{2(1-\lambda)(1-\lambda^2)}{\pi}-\frac{C_4}{C_L}\right]\sigma^2-(1-\lambda)\frac{C_4}{C_L}\sigma^3 \tag{27}$$

Unlike the spanwise load distribution for the pointed-tip wing, the load distribution for the finite-taper wing cannot be compared with an elliptical distribution for all wings but must be compared separately for each example investigated because of the form of equations (27) and (21b). The elliptical distribution is still given by equation (10).

NUMERICAL COMPUTATIONS

DEVELOPMENT OF FORM FOR COMPUTATION

After numerical values have been found for the constants C_1/C_L, C_2/C_L, C_3/C_L, and C_4/C_L, these values are used with equations (4), or rather with the numbers in table I computed from these equations, to find the z-displacement corresponding to each component of the pressure distribution. The four displacements are then added to produce the final shape of the warped wing. In principle this process is straightforward so that in practice it may be reduced to routine computation. A form suitable for such computation is now developed. The particular form presented is one such that, at a given spanwise station σ, the z-ordinate as a fraction of the local chord c is given as a function of x'/c, the fractional distance behind the leading edge of the local chord. As a typical example, the z-ordinate corresponding to the second term of equation (2) is considered. From equation (4b) the following relation is written:

$$\frac{m}{C_L}\frac{z_2}{c}=R_2\frac{C_2}{C_L}\frac{mc_r}{s}\left(\frac{x}{c_r}\right)^2\left(\frac{c_r}{c}\right)^2\frac{c}{c_r}$$

The following geometrical relations are easily verified:

$$\frac{x}{c_r}=[1-\sigma(1-\lambda)]\frac{x'}{c}+\frac{\sigma(1-\lambda)}{1-k}$$

$$\frac{c}{c_r}=1-\sigma(1-\lambda)$$

$$\frac{mc_r}{s}=\frac{1-k}{1-\lambda}$$

so that

$$\frac{m}{C_L}\frac{z_2}{c}=R_2\frac{C_2}{C_L}\frac{(1-k)[1-\sigma(1-\lambda)]}{1-\lambda}\left\{\frac{x'}{c}+\frac{\sigma(1-\lambda)}{(1-k)[1-\sigma(1-\lambda)]}\right\}^2$$

Now if A_0 is defined as

$$A_0=\frac{\sigma(1-\lambda)}{(1-k)[1-\sigma(1-\lambda)]}$$

then

$$\frac{\sigma}{A_0}=\frac{(1-k)[1-\sigma(1-\lambda)]}{1-\lambda}$$

and it can be shown that

$$\frac{A_0}{r}=\frac{x'}{c}+\frac{\sigma(1-\lambda)}{(1-k)[1-\sigma(1-\lambda)]}=\frac{x'}{c}+A_0 \tag{28}$$

so that

$$\frac{m}{C_L}\frac{z_2}{c}=R_2\frac{C_2}{C_L}\frac{\sigma}{A_0}\left(\frac{A_0}{r}\right)^2 \tag{29}$$

Thus, at a particular spanwise station σ on a given wing, z_2/c is a function only of r (since R as a function of r is known from table I). From equation (28), x'/c is also a function of r; thus,

$$\frac{x'}{c}=\frac{A_0}{r}-A_0$$

so that z_2/c can be calculated for various values of x'/c. By experience, it has been found that the most satisfactory way of choosing values of r to use in the computations is to plot, for the particular wing under consideration, x'/c against r (for the various values of σ) from equation (30). Only values of x'/c between 0 and 1 are of interest. This fact determines, for each σ, the range of r to be used, and from the values of r used as arguments in table I those which give a satisfactory distribution of points along the chord are chosen. Relations similar to equation (29) for the other z-components can be derived; these relations are

$$\left.\begin{aligned}\frac{m}{C_L}\frac{z_1}{c}&=R_1\frac{C_1}{C_L}\frac{A_0}{r}\\ \frac{m}{C_L}\frac{z_3}{c}&=R_3\frac{C_3}{C_L}\frac{\sigma}{A_0}\left(\frac{A_0}{r}\right)^2\\ \frac{m}{C_L}\frac{z_4}{c}&=R_4\frac{C_4}{C_L}\left(\frac{\sigma}{A_0}\right)^2\left(\frac{A_0}{r}\right)^3\end{aligned}\right\} \tag{31}$$

The amount of warp is seen to be directly proportional to C_L and inversely proportional to m (for a given n).

For some purposes, the wing shape can be more conveniently expressed in terms of z/c_r and x/c_r rather than in terms of z/c and x'/c. This conversion is easily made by use of the following equations:

$$\left.\begin{aligned}\frac{z}{c_r}&=[1-\sigma(1-\lambda)]\frac{z}{c}\\ \frac{x}{c_r}&=[1-\sigma(1-\lambda)]\frac{x'}{c}+\frac{\sigma(1-\lambda)}{1-k}\end{aligned}\right\} \tag{32}$$

TABLE II

COMPUTATIONAL FORM

$$\left[\begin{array}{cccc}\lambda=\text{———} & k=\text{———} & n=\text{———} & C_m=0 \text{ at } \frac{\overline{x'}}{\overline{c}}=\text{———}\\ m=\text{———} & M=\text{———} & C_L=\text{———} & \frac{C_L}{m}=\text{———}\\ \frac{C_1}{C_L}=\text{———} & \frac{C_2}{C_L}=\text{———} & \frac{C_3}{C_L}=\text{———} & \frac{C_4}{C_L}=\text{———}\end{array}\right]$$

$\sigma=$ ——— $\quad \frac{\sigma(1-\lambda)}{(1-k)[1-\sigma(1-\lambda)]}=A_0=$ ——— $\quad \frac{\sigma}{A_0}=$ ——— $\quad \left(\frac{\sigma}{A_0}\right)^2=$ ———

①	②	③	④	⑤	⑥	⑦	⑧	⑨	⑩	⑪	⑫	⑬	⑭	⑮	⑯	⑰
				From table I									z/c	x'/c	z/c_r	x/c_r
r (assumed)	$\frac{A_0}{①}$	$②^2\times\frac{\sigma}{A_0}$	$②^3\times\left(\frac{\sigma}{A_0}\right)^2$	R_1	R_2	R_3	R_4	$⑤\times②\times\frac{C_1}{C_L}$	$⑥\times③\times\frac{C_2}{C_L}$	$⑦\times③\times\frac{C_3}{C_L}$	$⑧\times④\times\frac{C_4}{C_L}$	$⑨+⑩+⑪+⑫$	$⑬\times C_L/m$	② − A_0	$⑭\times[1-\sigma(1-\lambda)]$	$⑮\times[1-\sigma(1-\lambda)]+\frac{\sigma(1-\lambda)}{1-k}$

The foregoing equations are embodied in table II, which is self-explanatory. This form has been used to compute several examples, some of which are discussed in the next section.

NUMERICAL EXAMPLES

Example I.—The first example chosen has the following characteristics:

$$n=0.6$$

$$k=0.6$$

$$\lambda=0$$

$$C_m=0 \quad \text{at} \quad \frac{\overline{x'}}{c}=0.25$$

This set of characteristics represents a sweptback wing, tapered to a point at the tips, with the center of pressure a little more than 50 percent of the mean aerodynamic chord ahead of the location for the corresponding flat wing. The lift coefficient, sweepback angle of the leading edge, and Mach number are not specified; the final amount of warp is directly proportional to the lift coefficient, and any combination of sweepback angle and Mach number that gives $n=0.6$ may be chosen.

The four constants are found from equations (12) to have the following values:

$$\frac{C_1}{C_L}=4.4530$$

$$\frac{C_2}{C_L}=-19.0819$$

$$\frac{C_3}{C_L}=15.9021$$

$$\frac{C_4}{C_L}=0.9071$$

Several values of σ are selected and, for these values, plots of x'/c against r are made from equation (30). Slide-rule accuracy is sufficient for these calculations, and only a few points need be taken to define the curves. The resulting curves for example I are shown in figure 7. These curves are used to pick values of r from table I. The corresponding values of R_1, R_2, R_3, and R_4 from table I are entered in table II, together with the other necessary data, and the indicated computations are carried out.

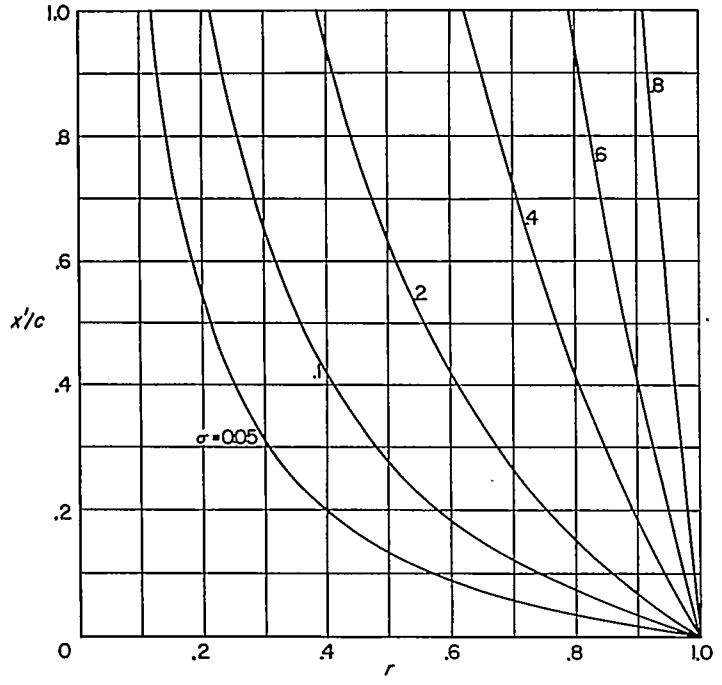

FIGURE 7.—Plot of x'/c against r for example I.

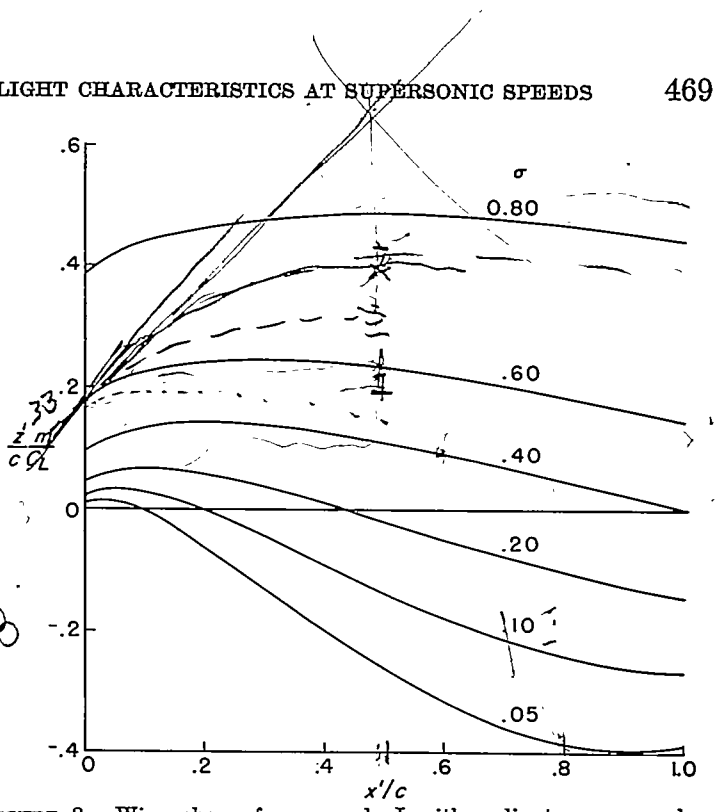

FIGURE 8.—Wing shape for example I with ordinates expressed as fractions of the local chord c.

The results of the computations are shown in figure 8, in which the ordinates are given as fractions of the local chord and the origin of the axes is at the leading edge of the local chord for each value of σ. Several features of the wing are evident from this form of presentation: namely, the reflex curvature of the airfoil sections near the center of the wing (the angle of attack is infinite at the center line), the disappearance of this reflex curvature at outboard sections, the relative twist between inboard and outboard sections, and the (variable) dihedral. A better picture of the actual wing is obtained by plotting the results as in figure 9. In order to give more physical meaning to the picture, the results have been plotted for a lift coefficient of 0.2 and a leading-edge sweep of 60° ($m=0.577$). This last value thus corresponds to a Mach number of 1.44 since n is equal to 0.6. There are two points worth mentioning with regard to figure 9. The first is that, within the accuracy of the linearized theory used in this report, an arbitrary $z(\sigma)$ may be added to the vertical ordinates without changing the aerodynamic characteristics of the wing. As pointed out in reference 1, this procedure is permissible so long as the resulting wing does not lie far from the $z=0$ plane (that is, modification of the wing shape by addition of a set of ordinates which depends only on σ (not on x) may be practiced in moderation). The practical significance of this point is that the wing shape may be modified by this procedure to simplify the problem of locating spars. The other point is that for most configurations the inboard stations of the wing, which are those having the largest warp, are buried within a fuselage and, therefore, present no structural problems. (The effect of the fuselage on the aerodynamic characteristics is discussed subsequently.)

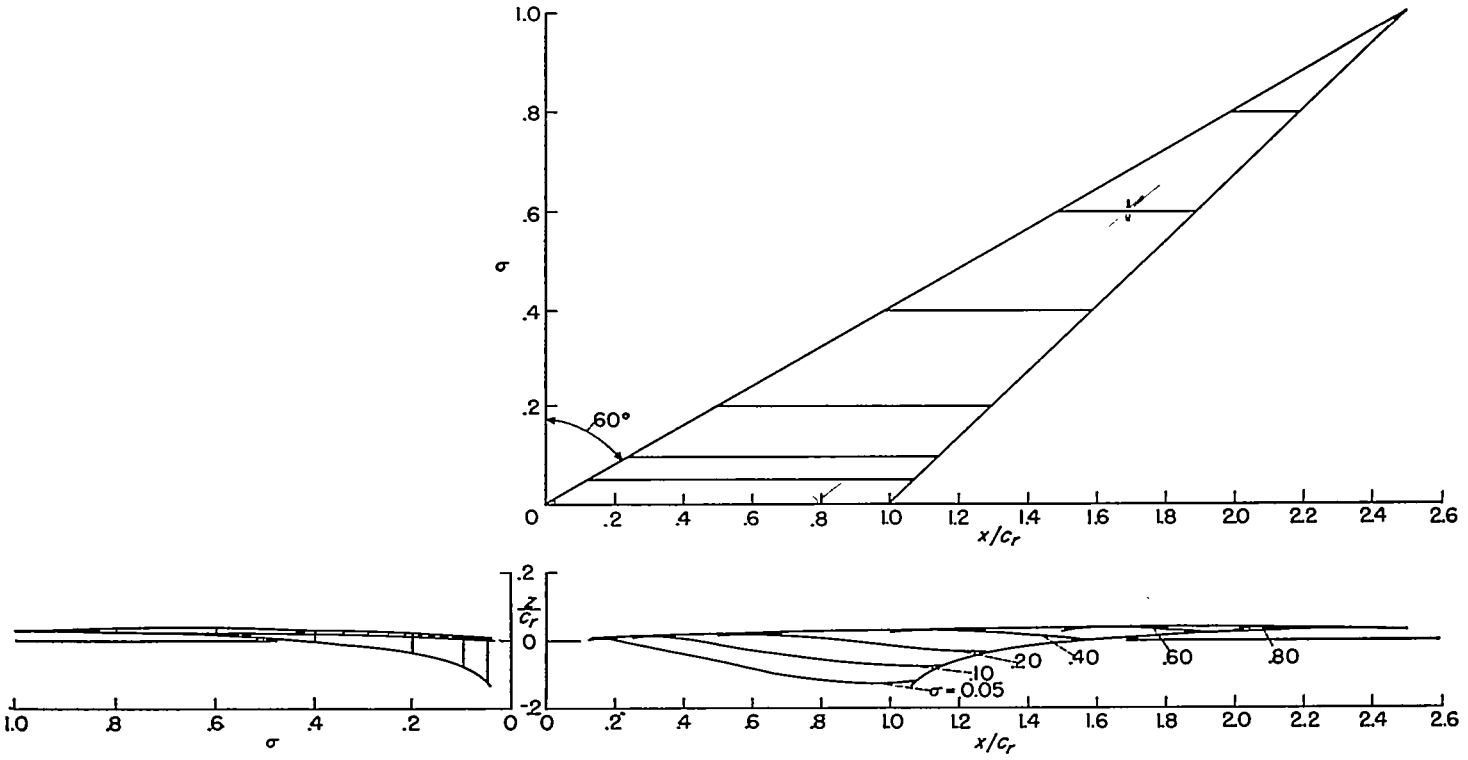

FIGURE 9.—Wing shape for example I with ordinates expressed as fractions of the root chord c_r. $C_L=0.2$; $m=0.577$; $M=1.44$.

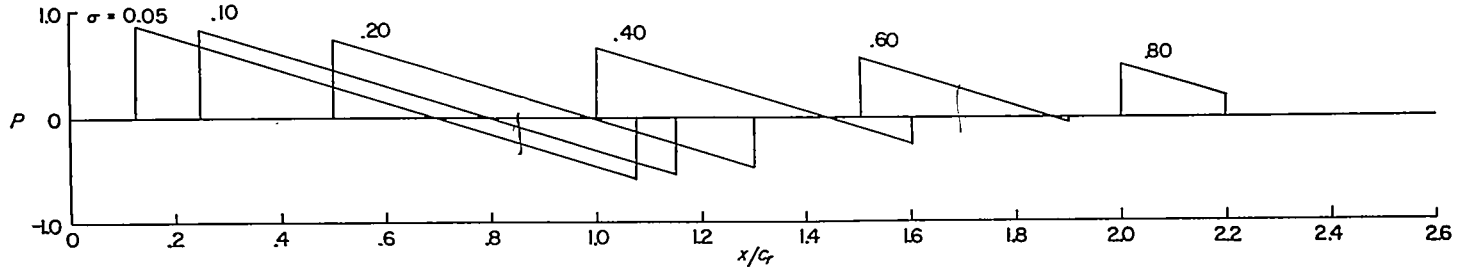

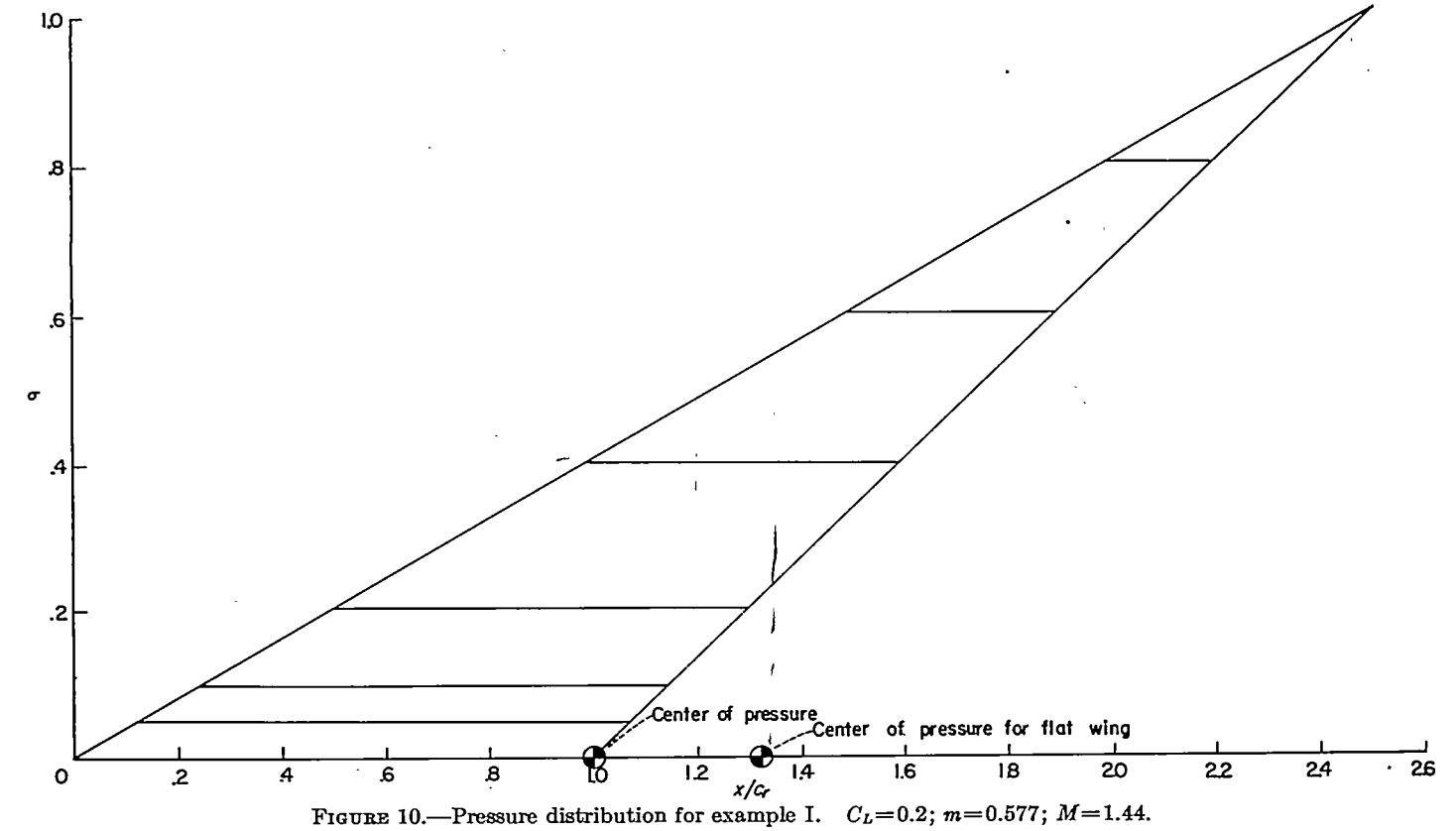

FIGURE 10.—Pressure distribution for example I. $C_L=0.2$; $m=0.577$; $M=1.44$.

This particular example and presumably others not too extreme should therefore be quite practical to build.

The pressure distribution for this example is shown in figure 10. Because of the far-forward specified location of the center of pressure, part of the wing carries negative lift. The spanwise distribution of load is that shown already in figure 6.

Example II.—The second illustrative example has the following characteristics:

$$n=0.8$$
$$k=0$$
$$\lambda=0$$
$$C_m=0 \quad \text{at} \quad \frac{\overline{x'}}{\bar{c}}=0.50$$

The values $k=0$ and $\lambda=0$ characterize a triangular wing. The center of pressure is at the same point as the center of pressure of the corresponding flat wing. The purpose of the present design is to show the kind of warp that might produce a wing with essentially the same center of pressure and spanwise load distribution as the flat triangle but without the steep pressure gradients that are known to promote leading-edge separation on the flat triangle, at least at low Reynolds numbers. A constant-pressure triangular wing, of course, has the same center-of-pressure location as a flat triangle and has no adverse pressure gradients, but the spanwise load distribution of such a wing is triangular rather than elliptical.

The method of computation is much the same as that used in the previous example. The principal difference is that equations (14), rather than equations (12), may be used to

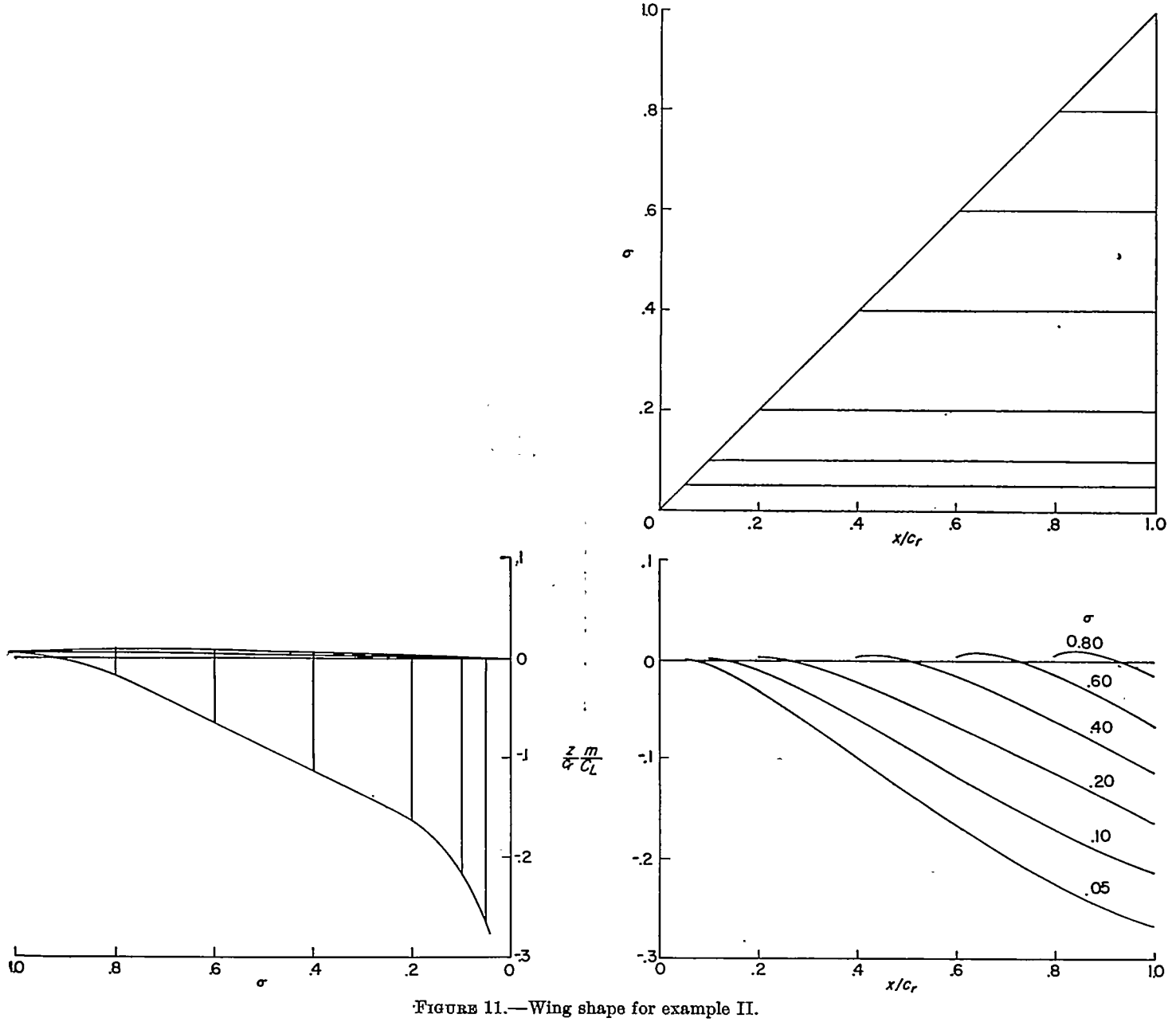

FIGURE 11.—Wing shape for example II.

find the following values for the four constants:

$$\frac{C_1}{C_L}=1.0907$$

$$\frac{C_2}{C_L}=-0.9082$$

$$\frac{C_3}{C_L}=1.0907$$

$$\frac{C_4}{C_L}=0.9071$$

The results of computations made with tables I and II are presented in figure 11. These plots clearly depict a wing the main part of which is almost flat and which has a turned-down leading edge, a small twist from root to tip, and almost constant dihedral angle along the span. For ease of manufacture, this dihedral can be removed without affecting the aerodynamic characteristics very much. (See the discussion of this point under example I.) The pressure distribution is shown in figure 12; the chordwise gradients of pressure are not large. The spanwise load distribution is again given by figure 6.

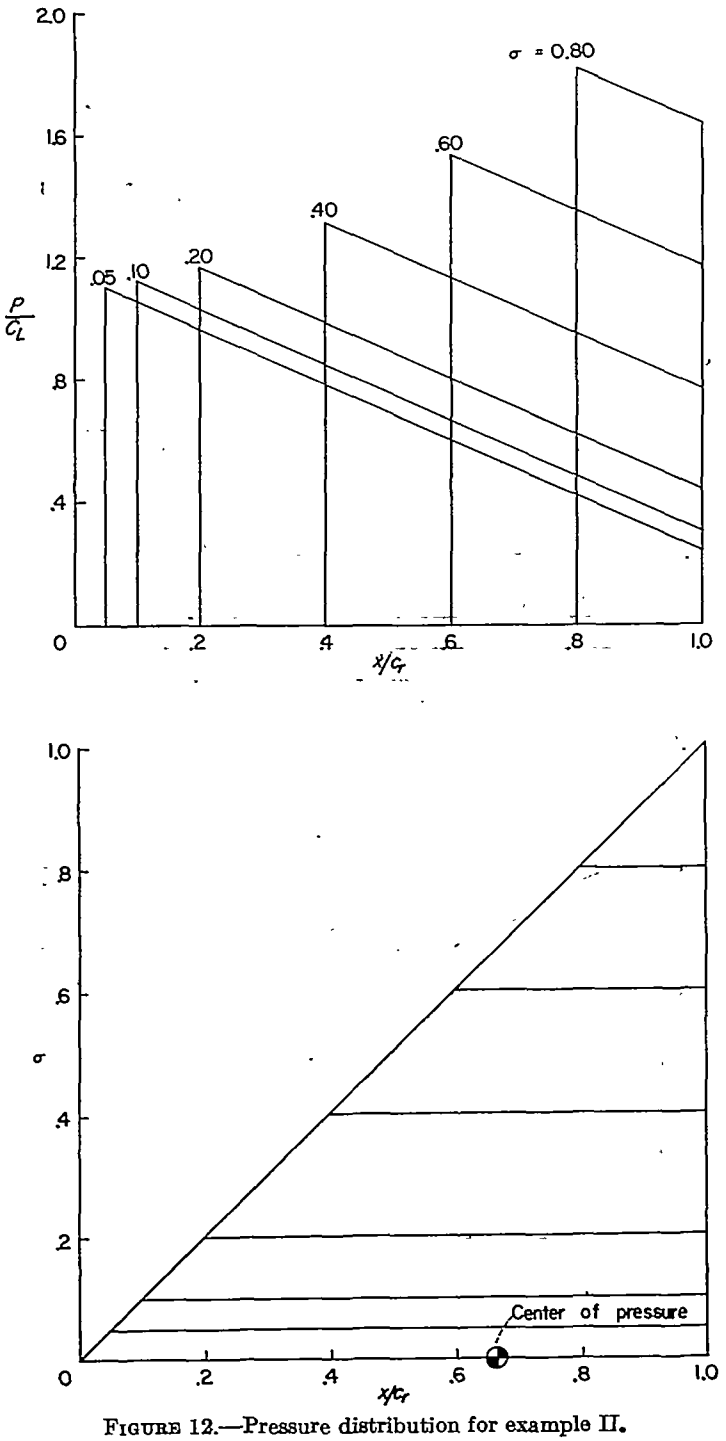

FIGURE 12.—Pressure distribution for example II.

Example III.—The third example chosen is a wing with finite taper, characterized by the following conditions:

$$n=0.7$$

$$k=0.6$$

$$\lambda=0.4$$

$$C_m=0 \quad \text{at} \quad \frac{\overline{x'}}{\overline{c}}=0.25$$

These values are substituted into equations (18), (20), and (26) to obtain the following values:

$$\frac{x_0}{c_r}=0.82857$$

$$A=0.05861$$

$$B=0.12308$$

$$C=0.20986$$

Substitution of these values into equation (24) gives

$$\frac{C_4}{C_L}=-0.1814$$

Substitution of this value into equation (25) gives

$$\frac{C_3}{C_L}=4.7438$$

The remaining constants are obtained by substitution of this value of C_3/C_L into equations (22) and (23); thus,

$$\frac{C_2}{C_L}=-5.2614$$

$$\frac{C_1}{C_L}=2.6451$$

From this point the method of calculation is the same as that used in the two previous examples: suitable values of r are chosen, and the form of table II is followed to arrive at values for the wing ordinates. The resulting wing shape is shown in figure 13 together with the pressure distribution; the results have been plotted for a lift coefficient of 0.4 and a leading-edge sweep of about 59° ($m=0.6$), corresponding to a Mach number of 1.54. The center-of-pressure location shown in the figure for the flat wing was found from reference 5. The wing shape is not extreme, and the previous remarks concerning the removal of the dihedral angle apply equally well to this case so that the wing can be built feasibly. The pressure plot shows the result of the assumption regarding the pressure in the tip region.

The following spanwise load distributions are found from equations (27) and (21b):

For $0 \leqq \sigma \leqq 0.795$,

$$\frac{cc_l}{c_r C_L}=0.891-0.502\sigma^2+0.109\sigma^3$$

For $0.795 \leqq \sigma \leqq 1$,

$$\frac{cc_l}{c_r C_L} = 2.82 - 2.44\sigma - 0.49\sigma^2 + 0.11\sigma^3$$

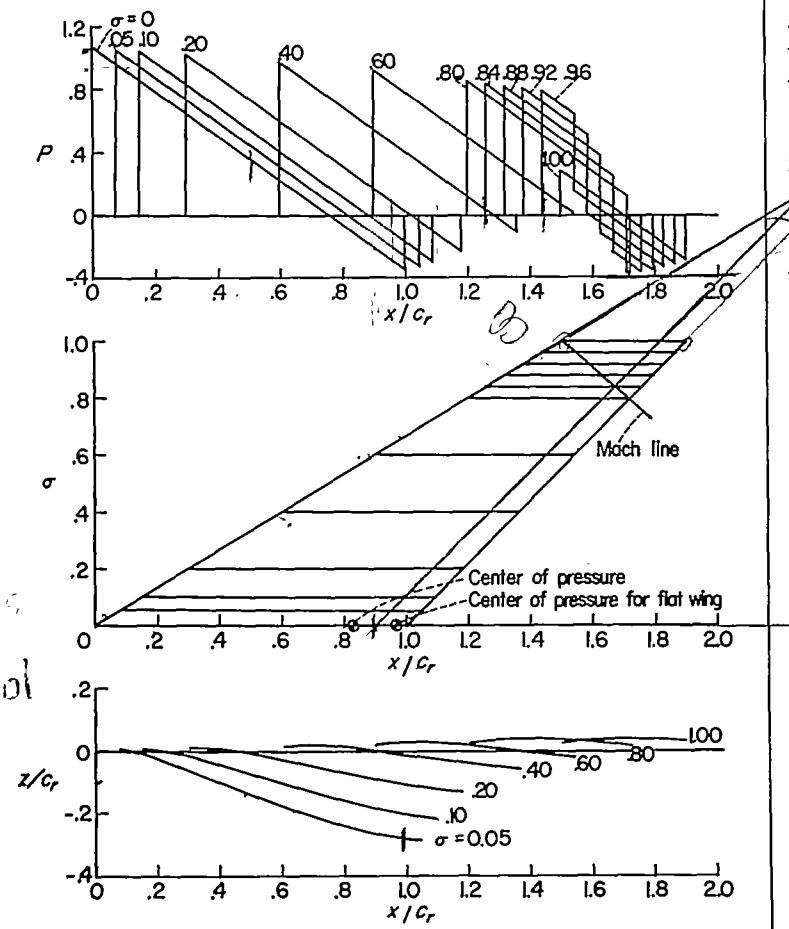

FIGURE 13.—Wing shape and pressure distribution for example III. $C_L=0.4$; $m=0.6$; $M=1.54$.

These equations are plotted in figure 14, which also shows an elliptical load distribution for comparison. The load distribution for the example being discussed is a fair approximation to the ellipse so that no large drag increase relative to the flat wing is to be expected as a result of the specified forward location of the center of pressure. As a matter of fact, the spanwise load distribution of the flat wing is itself not elliptical, so that the drag of the warped wing might well be less than that of the flat wing.

NOTES ON PRACTICAL APPLICATION

Range of applicability.—The method described in the preceding sections is directly applicable to wing plan forms of the types shown in figure 1. The locations of the various Mach lines shown in the figure relative to the leading and trailing edges and relative to the center line are significant. The leading edge must be subsonic and the trailing edge must be supersonic; these conditions are expressed by the following inequality:

$$1 \geqq n \geqq |k| \tag{33}$$

For the case of plan forms with finite tips ($\lambda \neq 0$), the Mach line from the leading edge of one tip must not cross over to the opposite wing panel. This condition is expressed by the following inequality:

$$n \geqq \frac{\lambda - k}{1 - \lambda} \tag{34}$$

In addition, because of the approximate nature of the assumption regarding the pressure in the tip region, cases in which the tip region covers a large part of the wing should be viewed with caution.

Computing time.—The exact time required to compute a given example depends on such factors as whether λ or k or both are equal to zero and the number of points taken to define the wing surface. The following time estimates are given as representative of those required by using a manually operated calculating machine. To calculate the constants, ½ to 1 hour is required, and to calculate eight spanwise stations, with 14 points along the chord at each station, 8 to 12 hours.

Body effect.—In the derivation of the present method, the wing has been considered as isolated; whereas, in practice it is usually mounted on a body, on which may also be mounted a tail. The available information, both theoretical and experimental, is not yet sufficient to allow an accurate quantitative prediction of the effect of the body for the general case. (See refs. 6 and 7 for a discussion of the problem.) Some qualitative estimates can be made, and by reference to whatever experimental data may be available for configurations resembling the particular example under consideration rough quantitative corrections can be applied for the effect of the body. If the wing is mounted on the body so that the chord line at the juncture is parallel to the body center line, then the lift of the combination when the wing is at its design position with respect to the free stream will probably be close to the sum of the lifts of the isolated wing and the isolated body. If, however, the two are connected so that when the wing is at its design position with respect to the free stream the body is at zero angle of attack,

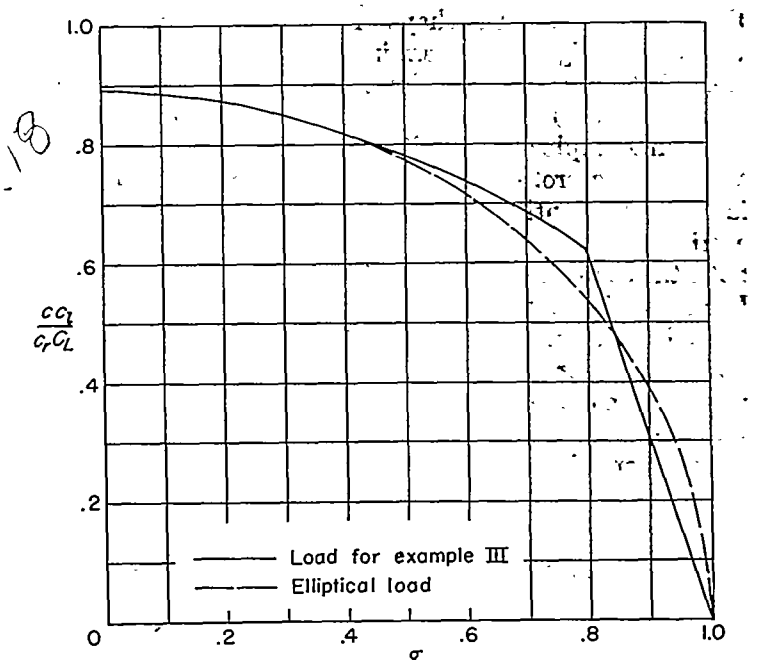

FIGURE 14.—Spanwise load distribution for example III compared with elliptical load distribution.

then the lift of the combination will probably be somewhat less than the design lift of the wing. In all cases, the center of pressure will probably be somewhat more rearward than that calculated when only the isolated components are considered. If these foregoing statements, which are obviously conjectural in nature, are accepted, then some allowance can be made for the effect of the body by adjusting the design conditions of the wing. The body-interference problem is neither different nor more serious for the warped wings considered in this report than for conventional flat wings, and all the preceding remarks apply equally well (or poorly, as the reader may judge for himself) to both types of wings.

Off-design operation.—In the course of a flight, the wing may be required to fly at the design Mach number at attitudes other than that for which it was designed. Within the limits of the linearized theory used in the analysis, the principle of superposition applies. The lift (and pitching moment) of the warped wing at an attitude different from the design condition is therefore simply the design lift and pitching moment plus (or minus) the lift and pitching moment of a flat wing of the same plan form at an angle of attack equal to the angular deviation of the warped wing from its design attitude. When the wing is required to operate at Mach numbers other than the design value, however, no simple method is available for estimating the change in aerodynamic characteristics, and even to calculate the properties by the use of the linearized theory is a practicably impossible job. An experimental test is the only way to find the answer.

Applicability to other problems.—Although the derivation of the complete method has been limited to wings of the types shown in figure 1, with approximately elliptical span loads, the basic results presented in equation (4) and table I are applicable to other wings as well. For example, a derivation similar to that presented in this report could be made for sweptback wings with cross-stream tips, such as that shown in figure 9 of reference 3. It is also conceivable that in some cases the shape of the spanwise-load-distribution curve might be determined by some condition other than that of low induced drag. The information presented in equations (4) and table I could be applied to such cases.

As an example of an application of the basic data of equations (4) to a problem of a type different from that discussed in the section entitled "Numerical Examples", the design of a triangular wing with approximately elliptical loading in both the spanwise and the chordwise directions is discussed. For convenience, this wing is called example IV. (In ref. 8, Jones has shown that, for a lifting surface of narrow proportions lying near the center of the Mach cone, the minimum value of the drag due to lift is achieved when both the spanwise and the chordwise loadings are elliptical.)

The chordwise load distribution is found from integration of equation (2) to be given by the following equation:

$$\frac{\text{Local lift}}{\text{Total lift}}=\frac{C_1}{C_L}\frac{x}{c_r}+\left(\frac{C_2}{C_L}+\frac{1}{2}\frac{C_3}{C_L}\right)\left(\frac{x}{c_r}\right)^2+\frac{1}{3}\frac{C_4}{C_L}\left(\frac{x}{c_r}\right)^3 \quad (35)$$

If, as in the previous examples, the conditions of equations (11) are applied to equation (9), then the spanwise load distribution is given by equation (15), and the values of C_1/C_L, C_2/C_L, and C_4/C_L are those of equations (14): namely,

$$\frac{C_1}{C_L}=\frac{C_3}{C_L}$$

$$\frac{C_2}{C_L}=\frac{4}{\pi}-2\frac{C_3}{C_L}$$

$$\frac{C_4}{C_L}=6-\frac{16}{\pi}$$

Substitution of these values into equation (35) gives the following equation for the chordwise load distribution:

$$\frac{\text{Local lift}}{\text{Total lift}}=\frac{C_3}{C_L}\frac{x}{c_r}+\left(\frac{4}{\pi}-\frac{3}{2}\frac{C_3}{C_L}\right)\left(\frac{x}{c_r}\right)^2+\left(2-\frac{16}{3\pi}\right)\left(\frac{x}{c_r}\right)^3$$

The chordwise load is now specified to be zero at the trailing edge $\left(\frac{x}{c_r}=1\right)$. This procedure gives the following value for C_3/C_L:

$$\frac{C_3}{C_L}=4-\frac{8}{3\pi}$$

and the chordwise load becomes

$$\frac{\text{Local lift}}{\text{Total lift}}=\left(4-\frac{8}{3\pi}\right)\frac{x}{c_r}-\left(6-\frac{8}{\pi}\right)\left(\frac{x}{c_r}\right)^2+\left(2-\frac{16}{3\pi}\right)\left(\frac{x}{c_r}\right)^3 \quad (36)$$

The load distribution given by equation (36) is compared with an ellipse in figure 15. The spanwise load distribution is also repeated from figure 6 for the sake of easy comparison.

The wing shape is readily calculated from tables I and II and is shown in figure 16 for $C_L=0.2$, $M=1.2$, and $n=0.3$.

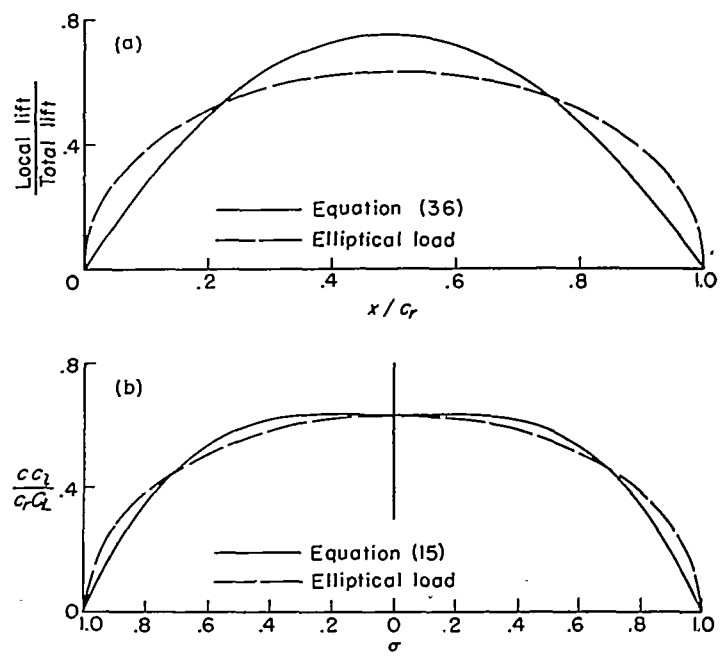

(a) Chordwise load.
(b) Spanwise load.

FIGURE 15.—Load distribution for example IV.

The drag coefficient for these conditions has been found by graphical integration to be approximately $C_D=0.0081$. The drag coefficient of a flat wing at the same conditions is 0.0091 if full leading edge suction is assumed or 0.0161 if no leading-edge suction is assumed (no leading-edge suction has been assumed for the warped wing).

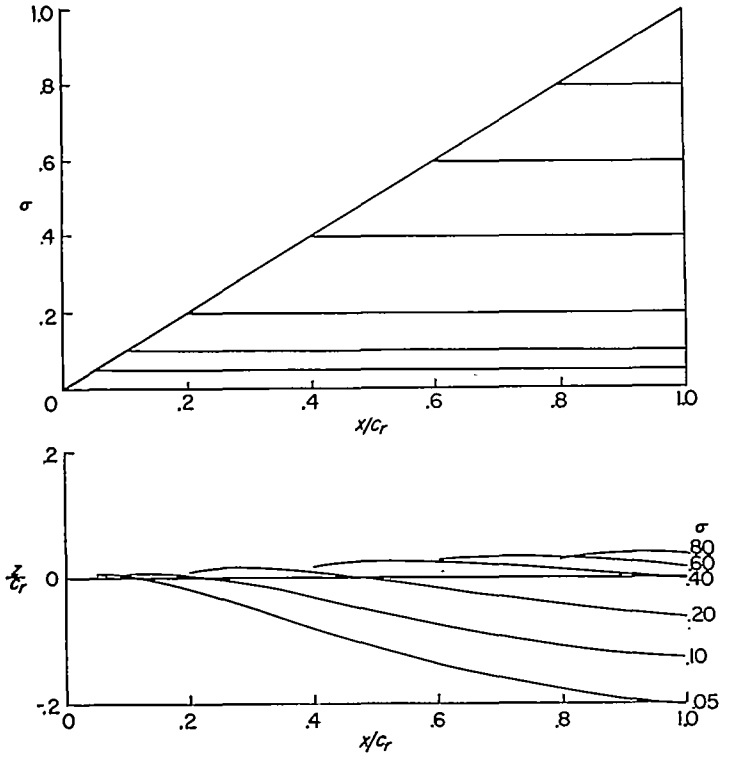

FIGURE 16.—Wing shape for example IV. $C_L=0.2$; $M=1.2$; $n=0.3$.

CONCLUDING REMARKS

A method has been presented for designing a sweptback wing to have certain specified flight characteristics at supersonic speeds. For example, a wing of given plan form, operating at a given supersonic Mach number, may be designed to have a specified lift coefficient, a specified center of pressure, and a nearly elliptical spanwise load distribution. As an aid in the calculations required for any specific case, certain basic data and a computational form are presented as tables. The procedure is illustrated by several examples.

LANGLEY AERONAUTICAL LABORATORY,
NATIONAL ADVISORY COMMITTEE FOR AERONAUTICS,
LANGLEY FIELD, VA., *May 11, 1951.*

REFERENCES

1. Baldwin, Barrett S., Jr.: Triangular Wings Cambered and Twisted To Support Specified Distributions of Lift at Supersonic Speeds. NACA TN 1816, 1949.
2. Martin, John C.: The Calculation of Downwash Behind Wings of Arbitrary Plan Form at Supersonic Speeds. NACA TN 2135, 1950.
3. Cohen, Doris: The Theoretical Lift of Flat Swept-Back Wings at Supersonic Speeds. NACA TN 1555, 1948.
4. Malvestuto, Frank S., Jr., Margolis, Kenneth, and Ribner, Herbert S.: Theoretical Lift and Damping in Roll at Supersonic Speeds of Thin Sweptback Tapered Wings With Streamwise Tips, Subsonic Leading Edges, and Supersonic Trailing Edges. NACA Rep. 970, 1950. (Supersedes NACA TN 1860.)
5. Malvestuto, Frank S., Jr., and Hoover, Dorothy M.: Lift and Pitching Derivatives of Thin Sweptback Tapered Wings With Streamwise Tips and Subsonic Leading Edges at Supersonic Speeds. NACA TN 2294, 1951.
6. Lagerstrom, P. A., and Van Dyke, M. D.: General Considerations About Planar and Non-Planar Lifting Systems. Rep. No. SM–13432, Douglas Aircraft Co., Inc., June 1949.
7. Lagerstrom, P. A., and Graham, M. E.: Aerodynamic Interference in Supersonic Missiles. Rep. No. SM–13743, Douglas Aircraft Co., Inc., July 1950.
8. Jones, Robert T.: The Minimum Drag of Thin Wings in Frictionless Flow. Jour. Aero. Sci., vol. 18, no. 2, Feb. 1951, pp. 75–81.